
Doctoral Dissertations

Student Theses and Dissertations

Fall 2014

Investigation of projectile coherence effects in fully differential studies of 75 keV proton - H₂ collisions

Sachin Sharma

Follow this and additional works at: https://scholarsmine.mst.edu/doctoral_dissertations



Part of the [Physics Commons](#)

Department: Physics

Recommended Citation

Sharma, Sachin, "Investigation of projectile coherence effects in fully differential studies of 75 keV proton - H₂ collisions" (2014). *Doctoral Dissertations*. 2357.

https://scholarsmine.mst.edu/doctoral_dissertations/2357

This thesis is brought to you by Scholars' Mine, a service of the Missouri S&T Library and Learning Resources. This work is protected by U. S. Copyright Law. Unauthorized use including reproduction for redistribution requires the permission of the copyright holder. For more information, please contact scholarsmine@mst.edu.

**INVESTIGATION OF PROJECTILE COHERENCE EFFECTS IN FULLY
DIFFERENTIAL STUDIES OF 75 KEV PROTON – H₂ COLLISIONS**

by

SACHIN SHARMA

A DISSERTATION

**Presented to the Faculty of the Graduate School of the
MISSOURI UNIVERSITY OF SCIENCE AND TECHNOLOGY**

In Partial Fulfillment of the Requirements for the Degree

**DOCTOR OF PHILOSOPHY
in
PHYSICS**

2014

**Approved
Michael Schulz, Advisor
D. H. Madison
J. L. Peacher
Y. S. Hor
H. K. Lee**

© 2014

Sachin Sharma

All Rights Reserved

PUBLICATION DISSERTATION OPTION

This dissertation has been prepared as a collection of publications in the style utilized by the Physical Review A and the Journal of Physics B. Three out of four articles have been published, pages 57-73 have been submitted in the Physical Review A. The Introduction in Section 1 and the Conclusions in Section 2 have been added for purposes normal to dissertation writing.

ABSTRACT

Fully differential cross sections (FDCS) have been measured for single ionization of H_2 by 75 keV proton impact with varying transverse coherence length of the projectiles. As reported in recent years, the scattering angle dependence of the doubly differential cross sections (DDCS) are significantly affected by the projectile coherence properties. The interference structures were observed for the coherent beam, however were absent for an incoherent beam. Interestingly, the FDCS measurements for fixed momentum transfer do not suggest significant differences between the coherent and incoherent cross sections. However, for the FDCS with fixed recoil-ion momentum, clear differences between the two has been established. This suggests that the momentum-transfer vector determines the phase angle in the interference term, which is the ratio between coherent and incoherent cross sections. Earlier, the phase angle entering in molecular two-center interference was believed to be determined by the recoil-ion momentum vector.

Recently, a theoretical study was reported which acknowledges that the measured DDCS mentioned above are affected by projectile coherence effects, however, suggests that this should not be seen as wave-packet (de)coherence effect. While our data do not disprove this assertion entirely, this theoretical analysis did not pass an experimental test proposed by its authors and performed within the research project for this thesis.

ACKNOWLEDGMENTS

Firstly, I would like to thank my family for an unconditional support on all the decisions I have made in my life so far. You have always been inspiring and I would never have achieved this without you. It was difficult decision to move that far from home. I consider myself very fortunate to meet my advisor, Dr. Schulz. You have always been a mentor and a guardian at the same time. I would always hope to be as hard-worker and professional like you. I would like to thank my mentor, Mr. Ramesh Dutt for all the support. I would also like to thank Dr. Ahmad Hasan for helping me with electronic equipment and data analysis. You have always been very humble and friendly. I would like to thank Dr. D. H. Madison, Dr. Jerry Peacher, Dr. P. E. Parris, Dr. G. Wilemski and Dr. Y. S. Hor for fruitful discussions. Thank you Dr. D. Waddill, Pam, Russ, Ronnie and Jan. You have been very supportive throughout my time here. Thank you very much Thusitha for your contribution. Also, thank you Amrita, Kisra, Hari, Uttam, Elizabeth, Basu and Sudip. I had a wonderful time all these years because of you guys. I would like to thank my best buddies; Rubal, Bhanu, Vimal, G. P. and Abhinav. I could only imagine having such a wonderful time again with you all.

Finally, thank you Shivani for constant encouragement. My life has become complete after meeting you and I find myself luckiest to have you.

TABLE OF CONTENTS

	Page
PUBLICATION DISSERTATION OPTION.....	iii
ABSTRACT.....	iv
ACKNOWLEDGMENTS	v
LIST OF ILLUSTRATIONS.....	ix
 SECTION	
1. INTRODUCTION	1
 PAPER	
I. Projectile Coherence Effects in Electron capture by Protons Colliding with H ₂ and He.....	15
Abstract.....	15
Introduction.....	16
Experiment.....	19
Results and Discussion	22
Conclusions.....	32
Acknowledgments.....	34
References.....	35
II. Complete Momentum Balance in Ionization of H ₂ by 75 keV Proton Impact for Varying Projectile Coherence	38
Abstract.....	38
Introduction.....	39
Experiment.....	42

Results and Discussion	45
Conclusions.....	52
Acknowledgements.....	53
References.....	54
III. Fully Differential Study of Interference in Ionization of H ₂ by Proton Impact..	57
Abstract.....	57
Introduction.....	58
Experimental set-up	60
Results and discussion	63
Conclusions and outlook.....	70
References.....	72
IV. Triple Differential Study of Ionization of H ₂ by Proton Impact for Varying Electron Ejection Geometries	74
Abstract.....	74
Introduction.....	75
Experiment.....	77
Results and Discussion	80
Conclusions.....	87
Acknowledgements.....	88
References.....	89

SECTION	
2. CONCLUSIONS	93
BIBLIOGRAPHY.....	99
VITA.....	102

LIST OF ILLUSTRATIONS

SECTION 1

Figure 1.1 : Three-dimensional ejected electron momenta for ionization of He by 100 MeV/a.m.u. C ⁶⁺	6
--	---

PAPER I

Figure 1: Schematic diagram of the experimental setup.....	20
Figure 2: Differential cross sections as a function of scattering angle for nondissociative capture in 75 keV p + H ₂ collisions.....	21
Figure 3: Differential ratios between the cross sections for a coherent and an incoherent projectile beam as a function of scattering angle for 75 keV p+H ₂	24
Figure 4: Same as Fig. 2 for 25 keV p+H ₂	25
Figure 5: Same as Fig. 3 for 25 keV p+H ₂ (closed symbols) and 25 keV p+He (open symbols).....	26
Figure 6: Same as Fig. 2 for dissociative capture in 25 keV p + H ₂	29
Figure 7: Same as Fig. 3 for dissociative capture in 25 keV p + H ₂	30

PAPER II

Figure 1: DDCSs for a fixed energy loss of 30 eV as a function of the projectile scattering angle θ	42
Figure 2: DDCSs for a fixed energy loss of 30 eV as a function of the x component of the recoil (top) and electron (bottom) momentum.	43
Figure 3: DDCSs for a fixed energy loss of 30 eV as a function of the y component of the electron.....	45
Figure 4: DDCS for a fixed energy loss of 30 eV as a function of the z component of the recoil-ion (top) and electron (bottom) momentum.	46
Figure 5: Ratio between the DDCSs of Fig. 2 for large and small slit distances for the electrons (open symbols) and recoil ions (closed symbols).....	47
Figure 6: Ratio between the DDCSs for large and small slit distances as a function of scattering angle (closed symbols).	48

PAPER III

Figure 1: Schematic diagram of the experimental set-up.	61
Figure 2: Fully differential, three-dimensional angular distribution of the ejected electrons taken for the large (left panel) and small (right panel) slit distance and for a momentum transfer of 0.9 a.u.	63
Figure 3: Fully differential cross sections for electrons ejected into the scattering plane as a function of the polar emission angle.	65
Figure 4: Fully differential cross sections as a function of the azimuthal electron ejection angle for fixed polar angles of 15° (top panels), 35° (center panels), and 55° (bottom panels)	67
Figure 5: Fully differential cross section ratios between the large and small slit distance data of Fig. 4.	68

PAPER IV

Figure 1: Experimental (left panel) and theoretical (right panel) three-dimensional plot of the triple differential cross sections for the electron energy fixed at 14.6 eV and the magnitude of the momentum transfer fixed at 0.9 a.u.	80
Figure 2: Triple differential cross sections for electrons with an energy of 14.6 eV ejected into the scattering plane as a function of the polar electron emission angle.	81
Figure 3: Triple differential cross sections for electrons with an energy of 14.6 eV ejected along the surface of a cone with an opening angle of 35° (45° for $q = 1.86$ a.u.) as a function of the azimuthal electron emission angle.	83
Figure 4: Same as Fig. 2 for electron ejection into the perpendicular plane.	86

SECTION

1. INTRODUCTION

Atomic collision experiments have significantly contributed to laying the foundation of Modern Physics. Over a century ago, Rutherford achieved a major step in uncovering the structure of atoms and their constituents by studying collisions of alpha particles with gold atoms. Although, a thorough understanding of atoms had to await the development of Quantum Mechanics, which started more than fifteen years after Rutherford's experiment, his work led to the fundamentally important realization that atoms are essentially "empty". Furthermore, Rutherford was the first to recognize the analogy between the motion of the electrons about the nucleus of an atom and the solar system.

After decades of advancement in both experimental and theoretical research in the field, the structure of atoms is essentially understood, at least for atoms (or ions) containing only one electron. Many electron atoms still represent some challenges. These challenges are due to the fact that the Schrödinger equation is not analytically solvable for more than two mutually interacting particles, even if the underlying force(s) are precisely known. This difficulty is known as the "Few-Body Problem" (FBP) in Physics. As far as the properties of stationary atoms are concerned, accurate solutions can nevertheless often be obtained by using numerical methods like e.g. the Hartree-Fock

approach. However, our understanding of dynamic few body systems, like e.g. atomic fragmentation processes, is much less comprehensive.

Atomic collision experiments are particularly well suited for the study of the dynamic few-body problem, primarily, because of two core reasons [1, 2]. Firstly, the underlying electromagnetic force is essentially understood. In contrast, in nuclear physics experiments, this advantage does not hold because the strong and the weak forces are not nearly as well understood as the electromagnetic force. Therefore, it is usually not clear whether experiments test the theoretical description of the underlying force(s) or of the few-body dynamics. Secondly, the number of particles involved in a collision process can be controlled to a very small number. In contrast, condensed matter systems, for example, involve a very large number of particles of the order of Avogadro's number. Therefore, it is not possible to extract complete kinematic information on an individual particle level from the experiment. Rather, only statistically averaged or collective quantities can be measured. Hence, a potential lack of understanding of the few-body dynamics could be hidden ("averaged out") in the statistics over a very large particle number. In contrast, for atomic collisions the particle number is small (≈ 3 to 5) enough to make kinematically complete experiments feasible, i.e. experiments in which the complete momentum vector of every single particle in the system is determined.

In a collision process, a large variety of processes can occur e.g. electron capture, target ionization, excitation etc. The single ionization process represents an ideal case for the study of the few-body dynamics because there are at least three particles (the ejected electron, the recoiling target ion, and the scattered projectile) involved in the final state of the system. In contrast, processes like electron capture and excitation kinematically

represent a two-body system because the electrons remain bound to one of the collision partners), which makes it less sensitive to the few-body dynamics.

The most detailed information about ionization can be obtained from a kinematically complete experiment. This can be done by the complete momentum measurement of any two of the three final state collision fragments i.e. scattered projectile, ejected electron and recoiling residual target ion. As the initial state momentum is precisely known the momentum of the third fragment can be determined by the kinematic conservation laws. From such kinematically complete data the fully differential cross sections (FDCS) can be extracted, which provide the most comprehensive information about the collision process.

The field of charged particles collisions involves three segments i.e. collisions with electrons, positrons and with ions as projectiles. For electron impact collision experiments, the direct projectile momentum measurements are less tedious than for heavy ion impact collisions because the electrons are far less massive than ions. As a result, deflections after the interaction with the target atom or molecule are in the range of degrees (rather than sub-mrad in the case of ions) and therefore detection of both the projectile and the ejected electron can be done with sufficient angular resolution.

The very first FDCS measurements for the single ionization of helium by electron impact were performed more than four decades ago [3]. The results obtained were compared to calculations based on the elementary Lippmann - Schwinger equation. Initially, only marginal agreement between theory and experiment was achieved. However, for electron impact ionization, the developments of sophisticated non-

perturbative models finally resulted in very good agreement with experimental data more than two decades later, even close to threshold, which previously was regarded as a particularly challenging regime [4].

For heavy-ion projectiles, on the other hand, not only the projectile deflections are often in the sub milliradians (mrad) or even sub microradians (μrad) range, as mentioned above, but also the energy loss relative to the initial energy (which determines the magnitude of the final projectile momentum) is very small. In fact, for fast and/or heavy ions both the scattering angle and the energy loss are immeasurably small [6]. The FDCS measurements involving the direct momentum analysis of scattered projectile ions are only feasible for light ions of energies up to approximately 200 keV using the unique recoil-ion/projectile momentum spectrometer at Missouri S & T.

Before the relatively recent and substantial advancements in the FDCS measurement techniques, many experimental limitations persisted in the regime of kinematically complete experiments even for electron impact ionization studies [4, 8]. In order to obtain comprehensive and detailed information about the FDCS with large efficiencies, the momentum spectra of the collision fragments should ideally be measured with 4π solid angle. In the early experiments, this was not feasible and therefore FDCS measurements were rather limited in the accessible kinematic range. Because of the aforementioned additional problems, FDCS measurements for ion impact were not possible at all until about 15 years ago.

This changed dramatically with the development of Cold Target Recoil Ion Momentum Spectroscopy (COLTRIMS) in combination with two-dimensional position-

sensitive detection techniques [9-10]. With this method, it became feasible to measure the complete momentum vectors for the recoil ions with high resolution and large solid angle. For ion-impact collisions, because of the problems mentioned above, the direct measurement of projectile momentum spectra is only achievable for light ions at small and intermediate projectile energies. Therefore, in this regime the momentum of the ejected electron can be determined by directly measuring the projectile and the recoil-ion momentum vectors and applying the kinematic conservation laws. However, due to sub μ rad deflections for very large projectile energies (and/or heavy ions), the projectile momentum can only be determined by using reversed kinematics. Here, the electron and the recoil-ion momenta are directly measured and the conservation laws determine the deflected projectile momentum. Additionally, all the momentum measurements could be performed with nearly 4π solid angle and hence the accessible kinematic range of reaction dynamics was greatly enhanced. This dissertation, deals with light ion impact collisions at intermediate energies, where the direct projectile momentum measurement is still very challenging, but feasible.

An important parameter characterizing ion-atom collisions is the projectile charge to speed ratio “ η ”, which in the literature is known as the perturbation parameter. For collisions with large projectile energies, where η is very small compared to unity, measured FDCS have been fairly well reproduced by both perturbative and non-perturbative models [2, 5-7, 13-14]. But, this good agreement was achieved only for very specific kinematic regime i.e. when the electron is ejected into the scattering plane, which is the plane spanned by the initial projectile momentum vector p_0 and the momentum transfer vector q . For this specific regime even the First Born Approximation (FBA)

models reproduced experimental results satisfactorily. Thus, until about a decade ago it was believed that the collision dynamics, at least for very small η , was basically

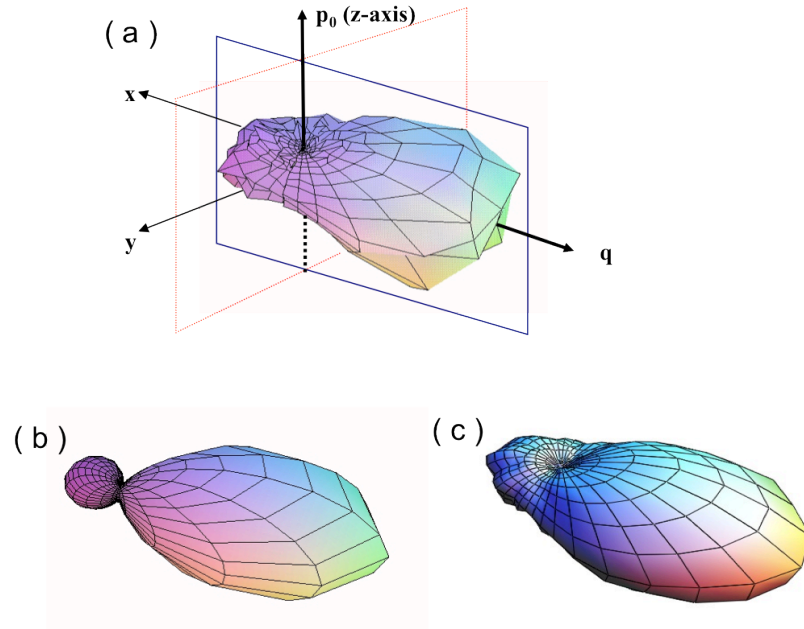


Figure 1.1: Three-dimensional ejected electron momenta for ionization of He by 100 MeV/a.m.u. C^{6+} . (a) Experiment (b) 3DW calculations (c) FBA convoluted with classical elastic scattering.

understood [1, 3, 18]. But then, with the advent of COLTRIMS, FDCS measurements outside the scattering plane also became feasible and, surprisingly, significant qualitative discrepancies for ion impact collisions were observed in this region [12-14].

In Fig. 1.1(a), a measured fully differential three-dimensional angular distribution of the ejected electrons is plotted for single ionization of He by 100 MeV/a.m.u. C^{6+} ions. The projectile momentum p_0 represents the direction of the incident projectile beam, which, conventionally, is the z-axis and q represents the direction of the momentum transfer vector, which is the vector difference of the initial and the final projectile

momentum. Fig. 1(b) shows the three-dimensional angular distribution of the ejected electron, based on the three-body distorted wave (3DW) calculations [19]. The 3DW model is a fully quantum mechanical model, which perturbatively treats higher-order contributions in all interactions within the various particle pairs in the collision system in the initial- and final-state wavefunctions.

Theory predicts a pronounced double peak structure separated by a distinct minimum at the origin (Fig. 1(b)), however, this minimum is almost entirely filled up in the experimental results (Fig. 1(a)). The larger peak in Fig. 1(b), which is in the direction of q , is known as the binary peak in the literature. The binary peak exists due to a binary interaction (i.e. the target nucleus remains passive) between the projectile and the electron to be ejected. The smaller peak in the direction opposite to q is known as the recoil peak. The recoil peak emerges due to the backscattering of the ejected electron (following the primary interaction with the projectile) because of its interaction with the target nucleus. Despite good agreement in the scattering plane, surprising discrepancies can be observed in the perpendicular plane, which is the plane perpendicular to the scattering plane that contains p_0 . All fully quantum mechanical models display similar discrepancies e.g. [13, 18-22]. In some of the theoretical papers it was reported that these discrepancies might merely be due to resolution effects [15, 16], but these claims were experimentally refuted soon after [17,18]. It was realized that the resolution effects suggested were only due to the incorrect target temperature used for the calculations, which was overestimated by an order of magnitude compared to the actual temperature realized in the experiments.

Surprisingly, a relatively simple semi-classical model Fig. 1(c) very nicely reproduced the experimental data in Fig. 1(a) [17, 18]. In this model, the FBA was convoluted with classical elastic scattering, between the projectile and the target nucleus, by the Monte Carlo Event Generator (MCEG) technique [17,18]. Initially, a theoretical event-file is generated. The event file consists of the momentum components of all collision fragments for a large number of ionization events simulated based on the FDCS calculated with the FBA, which does not account for the projectile – target nucleus interaction. Then this interaction was added retroactively by adding an appropriate momentum transfer, determined from a classical impact parameter approach, to the different momentum components in the event file, on an event-by-event basis. Moreover, the experimental resolution can also be modeled by this technique. Surprisingly, this model displayed much better agreement with the experimental data than fully quantum-mechanical calculations. This raised the question whether this unexpected success was fortuitous or whether it was indicative of some problem that all fully quantum-mechanical problems had in common and which for some reason did not affect the semi-classical approach based on the MCEG technique.

Recently, Egodapitiya et al. suggested that the discrepancies to fully quantum-mechanical calculations might be due to unrealistic assumptions regarding the projectile coherence properties [23]. As discussed earlier, these models share one fundamental feature; they all assume that the projectile is completely delocalized i.e. the wave-packet has an infinite width. Therefore, the projectile is theoretically presumed to be coherent to the target, however, experimentally it might not always be coherent. Particularly, in fast heavy ion collision experiments, the projectile wave-packet can rather be very well

localized due to the tiny de Broglie wavelength i.e. the wave-packet has a very small width, which can make the beam incoherent over the dimensions of the target atom.

One possibility to test a potential influence of the projectile coherence properties on the cross sections is to study ionization of molecular targets like e.g. H_2 . It is well established that the molecular two-center or Young double-slit type of interference can be observed in the projectile scattering angles dependence of the collision cross sections [24]. The indistinguishable diffraction of the incoming projectile wave from the two atomic centers can give rise to interference structures. Such interference structures were first predicted by Tuan and Gerjuoy [25] for a charge transfer process, where an electron from H_2 is captured by a proton and successively by Cohen and Fano for photoionization of electrons from molecular hydrogen, where the interference patterns were seen in the angular distribution of ejected electron spectrum [26]. For heavy ion collisions, the interference structures were first observed for electron capture from a molecular deuterium target by bare oxygen ions [27]. Similar effects were later observed for various electron impact experiments as well as heavy ion impact collision experiments with different diatomic targets [28-31]. Moreover, Schmidt et al. reported an experiment in which molecular, H_2^+ , projectiles were collided with a monoatomic target (He) [33]. They observed a pronounced interference structure in the transverse momentum transfer spectrum for dissociative electron transfer from the target to the H_2^+ ion and another similar experiment was reported very recently for a different reaction channel [34].

However, one essential requirement for the occurrence of molecular two-center interference is that the TCL should be larger than the inter-nuclear separation. In that case both atomic centers of the molecule are simultaneously illuminated by the incoming

projectile wave. If, on the other hand, the TCL is smaller than the internuclear separation then only one atomic center can be illuminated at a time and consequently no interference can occur. In 2000, Keller et al. reported an experimental study on diffraction of slow atomic projectiles from a periodic potential generated by laser field. They were able to control the TCL by changing the width of the collimating slit, using the well-established formulism in Optics, that $TCL = \lambda L/2a$, where λ is the de-Broglie wavelength of the projectile beam, L is the distance between the target and the collimating slits and a is the width of the collimating slits [36]. They thereby demonstrated that by varying the slit width (or distance to the target) it is possible to control whether or not an interference pattern is present in the measured angular distribution of the diffracted projectiles.

Egodapitiya et al. measured the doubly differential cross sections (DDCS), differential in the energy loss and in the solid angles of the projectiles, for both a coherent and an incoherent projectile beam [23]. They controlled the TCL by changing L , the distance between the target jet and the collimating slits. The collimating slit closer to the target i.e. the smaller TCL represented the incoherent projectile beam and the slit located farther away from the target i.e. the larger TCL represented the coherent projectile beam. They observed significant differences in the DDCS between the coherent and the incoherent projectile beam. The scattering angle dependence of the coherent DDCS appeared to be oscillating about the one for the incoherent DDCS. Also, quite remarkably, the DDCS for the incoherent projectile beam were found to be very similar to twice the DDCS measured for the atomic hydrogen target under similar experimental conditions [37].

In analogy to classical optics, the coherent cross sections can be expressed as the incoherent cross sections times the interference term (IT):

$$(DDCS)_{coherent} = (DDCS)_{incoherent} * IT \quad [1]$$

Therefore, IT can be written as the ratio between the coherent and the incoherent cross sections, and for molecular two-center interference is given by [28, 35]

$$IT = [1 + \cos(\mathbf{p}_{rec} \cdot \mathbf{D})] = [1 + \cos \delta] \quad [2]$$

if the molecular orientation is fixed. Here, \mathbf{p}_{rec} represents the recoil momentum vector and \mathbf{D} is the inter-nuclear separation vector. The term “ $\mathbf{p}_{rec} \cdot \mathbf{D}$ ”, in the above-mentioned equation, is the phase angle δ , which depends upon the orientation of the molecule relative to \mathbf{p}_{rec} . If the orientation of the molecule cannot be determined in the experiment, IT has to be averaged over all possible molecular orientations. For a random orientation this yields

$$IT = [1 + (\sin \delta) / \delta] \quad [3]$$

Although the experiment performed by Egodapitiya et al. in [23] illustrated coherence effects for H_2 (molecular target), it did not yet provide ultimate evidence that the discrepancies observed for ionization of He (atomic target) by C^{6+} in [1] are also due to projectile coherence effect. Very recently, Wang et al. performed an analogous experiment to $C^{6+} + He$ experiment [1] by keeping the same perturbation parameter η [38]. Moreover, the crucial feature of this experiment was that the projectile (proton) beam was much more coherent. Theoretically, both the experiments should result in

practically identical FDCS. However, in the $p + \text{He}$ case [38] the minimum at the origin appeared to be more pronounced relative to the $\text{C}^{6+} + \text{He}$ experiment [1] see Fig. 1.1). The minimum is a signature of destructive interference and the “filling up” of the minimum in the case of the C^{6+} projectiles can thus be associated with the incoherence of the projectile beam which results from the tiny de Broglie wave length of such a heavy and very fast ion.

Obviously, for an atomic target any coherence effects cannot be related to molecular two-center interference. Instead, it has been proposed that these effects are due to an atomic single-center path-interference. The coherent sum of first- and higher-order transition amplitudes, involving e.g. the projectile – target nucleus interaction, can give rise to such type of interference. The impact parameter dependence for the first- and higher-order contributions to the cross sections at a fixed scattering angle is usually quite different. This type of interference can therefore also be viewed as interference between different impact parameters leading to the same scattering angle.

The motivations for this dissertation were manifold. First, to investigate the projectile coherence effects for a different reaction channel, which were performed by measurements of singly differential cross sections (SDCS) for single electron capture from H_2 by 75 keV proton impact. The primary advantage of this particular reaction channel is that the entire momentum is transferred to the recoil ion. Therefore, the phase angle δ in the interference term is better defined. Additionally, unlike the ionization experiment [23], the coherent and the incoherent cross sections can be measured in the same experimental run and therefore the possibility of these effects being due to different experimental conditions can be ruled out.

As discussed earlier, for the ionization of He, Wang et al. reported the contraction of the momentum distribution at the origin due to higher transverse coherence length of the projectiles as compared to [1]. This contraction was proposed due to atomic-path interference. The SDCS measurements were performed for single electron capture from He and H₂ by 25 keV protons with varied coherence length. For He, this experiment provides a direct investigation of atomic-path interference, as two-center interference can be ruled out completely. However, for H₂, both types of interferences could be present. Therefore, one goal of this study was to see which type of interference could be observed or whether one is dominant over the other.

Despite the above-mentioned advantages of the single electron capture experiments in understanding the role of projectile coherence in a collision process there is one fundamental limit to the information one can obtain, in general, about the interference term. This is due to the fact that the single capture is kinematically a two-body process and the momentum is transferred entirely to the recoil-ion. Therefore, the phase angle in the interference term depends solely on \mathbf{p}_{rec} ($= \mathbf{q}$) i.e. in single capture it can not be distinguished whether δ depends primarily on \mathbf{p}_{rec} or \mathbf{q} . However, in the case of single ionization, which is a three-body process, momentum transfer is shared between the recoil-ion and the ejected electron and an experimental study on ionization can thus distinguish whether δ depends primarily on \mathbf{p}_{rec} or \mathbf{q} , since they are different.

Very recently, Feagin and Hargreaves reported a theoretical study on the coherence properties of the projectiles. They acknowledged that the projectile coherence properties can affect the cross sections, however, they argued that this should not be viewed as wave-packet (de)coherence. They claimed that the incoherent cross sections

could be reproduced by averaging the coherent cross sections over an entire range of angles subtended by the collimating slit at the target. In conclusion, they associated the loss of interference in the incoherent cross sections to the poor collimation of the projectile beam rather than wave-packet coherence. However, they suggested a test that can address the resolution effects, if any, between the coherent and the incoherent cross sections. They proposed that in the FDCS measurements, the projectile scattering angles could be measured directly and could also be deduced from the electron and recoil-ion momenta using conservation laws. Thus, for the collision events with same scattering angles, the effective collimation angle that slit subtends on the target reduce significantly and the coherent and incoherent DDCS should become indifferent.

In order to address above-mentioned issues, the FDCS were measured for single ionization of H_2 by 75 keV protons impact. Similar to the previous experiments, these measurements were also performed with both coherent and incoherent projectiles. Since these measurements provide all the momentum components involved in the collision process, the projectile coherence effects can be investigated for each momentum component distinctly. From the FDCS, more detailed analysis of the phase angle in the IT can be performed as their dependence on \mathbf{p}_{rec} and \mathbf{q} can be tested exclusively. Moreover, the DDCS can be deduced by averaging the FDCS appropriately, therefore, the projectile coherence effects for all momentum components belonging to each collision fragment can be studied distinctly. Currently, the FDCS measurements for ionization of H_2 with higher energy loss to the projectile are ongoing which can provide more insights to the projectile coherence effects.

PAPER**I. Projectile Coherence Effects in Electron capture by Protons Colliding with H₂ and He**

S. Sharma¹, A. Hasan^{1,2}, K.N. Egodapitiya^{1,†}, T. P. Arthanayaka¹, G. Sakhelashvili^{1,3}, and
M. Schulz¹

¹Department of Physics and LAMOR, Missouri University of Science & Technology,
Rolla, Missouri 65409, USA

²Department of Physics, UAE University, P.O. Box 17551, Alain, Abu Dhabi, United
Arab Emirates

³College of Arts and Sciences, Ilia State University, 0162 Tblisi, Georgia

Abstract

We have measured differential cross sections for single and dissociative capture for 25 and 75 keV protons colliding with H₂ and He. Significant differences were found depending on whether the projectile beam was coherent or incoherent. For 75 keV p + H₂ these differences can be mostly associated with molecular two-center interference and possibly some contributions from path interference. For 25 keV (both targets) they are mostly due to path interference between different impact parameters leading to the same scattering angles and, for the H₂ target, possibly some contributions from molecular two-center interference.

[†] Present address: Dept. of Physics, University of Virginia, 382 McCormick Rd, Charlottesville, VA 22904-4714

Introduction

To accurately calculate atomic scattering cross sections remains a very challenging task even after several decades of research. The basic underlying difficulty is that the Schrödinger equation is not analytically solvable for more than two mutually interacting particles. Therefore, elaborate numerical methods have been developed and reliable theoretical total cross sections are routinely obtained for a broad range of collisions systems and for a variety of processes (for reviews see e.g. [1,2]). In the case of ionization, differential ejected electron spectra can also be reproduced by theory with remarkable accuracy even at very large perturbation (projectile charge to speed ratio η) [3], which is considered to be a particularly challenging regime.

These successes sharply contrast with serious problems which arise when experimental and theoretical data are compared for cross sections differential in projectile parameters. For the same collision system for which measured differential electron spectra are nicely reproduced by theory (3.6 MeV/amu $\text{Au}^{53+} + \text{He}$, $\eta = 4.5$ [3]) severe discrepancies are observed in the double differential cross sections (DDCS) as a function of electron energy and projectile momentum transfer q [4]. In fully differential cross sections (FDCS) significant discrepancies were even observed for very small η (0.1) [5], for which the collision dynamics was thought to be essentially understood. The disagreement to experiment was particularly pronounced in fully quantum-mechanical calculations [e.g. 5-8], but amazingly if the interaction between the projectile and the target core (PI interaction) was treated classically or semi-classically good or at least improved agreement was achieved [9-12].

Numerous attempts were made to explain these discrepancies. Fiol and Olson [8] attributed them entirely to the experimental resolution. However, a more thorough analysis, based on more realistic parameters, revealed that the resolution can only account for a small fraction of the discrepancies [9,13]. Madison et al. [14] have pointed out that in their distorted wave approach the three-body final state wavefunction may not be accurate if all particles are close together. On the other hand, a non-perturbative approach, which is not affected by this problem, yielded essentially the same results [15]. Foster et al. [16] observed that for electron impact the calculations were very sensitive to the description of the screening of the target nucleus by the passive electron, but for ion impact at small η Voitkiv and Najjari [7] did not find a significant change with varying screening. Finally, one might expect that the presence of the second electron in the target atom could have a noticeable effect on the cross sections beyond merely screening the nucleus. For example, correlation between both electrons could be important or other reaction channels (like e.g. ionization plus excitation), not present for a one-electron target, could be stronger than expected. However, in recent experiments significant discrepancies between theory and experiment were found in the DDCS even for an atomic hydrogen target [17].

The key to resolving the puzzling discrepancies between theory and experiment, even for small η , was provided by new experimental developments. Earlier, path interference and molecular two-center interference of a single electron ejected in atomic collisions was predicted by theory [e.g. 18] and experimentally observed [e.g. 19-21]. More recently we demonstrated that in the scattering angle dependence of the DDCS for ionization in $p + H_2$ collisions an interference pattern, due to indistinguishable diffraction

of the projectiles from the two atomic centers of the molecule, was present for a coherent, but not for an incoherent projectile beam [22]. In analogy to classical optics the transverse coherence length Δr is determined by the geometry of a collimating slit placed before the target and the DeBroglie wavelength of the projectile wave λ by [23]:

$$\Delta r = \frac{1}{2} (L/a) \quad (1)$$

where a and L are the width of the collimating slit and its distance to the target. In optical Young double slit interference the requirement for transverse coherence is that Δr is larger than the double slit separation. In the case of ionization of H_2 the role of the slit separation is taken by the internuclear distance D in the molecule. The experiment of ref. [22] was performed for two different L corresponding to $\Delta r = 3$ and 0.4 a.u., respectively. With $D = 1.4$ a.u., the projectile beam was coherent for the larger and incoherent for the smaller value of Δr .

Furthermore, we proposed in [22] that the discrepancies between experiment and theory in the FDCS for ionization of He could be due to artificial path interference in the calculations. Consider, for example, the first-order amplitude, where the projectile only gets deflected from the target electron, and a second-order amplitude involving the interaction of the projectile with the target nucleus so that the projectile is deflected attractively (by the electron) and repulsively (by the nucleus). One would expect that for these two amplitudes different impact parameter ranges mainly contribute to the same scattering angle θ [24]. In the calculations, the coherent sum of both leads to an interference term. Indeed, this type of interference was recently found in perturbative calculations of FDCS for intermediate energy $p + He$ collisions [25]. However, an observable interference requires a coherent projectile beam. On the other hand, Δr

realized in the experiments is typically very small compared to atomic dimensions, especially for small η , and the interference term is then not observable. Recently, FDSC measurements were performed for small η at an ion storage ring, where coherent projectile beams can be prepared through electron cooling [26]. Indeed, in this study the discrepancies between experiment and theory observed for an incoherent beam are largely resolved.

The important role of the projectile coherence has been overlooked for decades of atomic collision studies and is still largely unexplored. The recent findings just represent the beginning of a new research direction in this field. A systematic study of the role of the projectile coherence, extending the initial measurements to a broad range of collision systems and scattering processes, is necessary to gain a complete understanding of interference phenomena in atomic collisions. In this article, we report results of such studies on electron capture in collisions of protons with He and H₂ which confirm the important role of the projectile coherence.

Experiment

A sketch of the experimental set-up is shown in Fig. 1. A proton beam was generated with a hot cathode ion source and accelerated to energies of 25 and 75 keV. A pair of collimating slits, each with a width of 0.15 mm, was placed in front of the target region at a distance $L_x = 6.5$ cm in the x-direction and $L_y = 50$ cm in the y-direction. The beam intersected with a very cold ($T \approx 2$ K) H₂ or He beam from a supersonic jet. After the collision, the projectiles were charge-state analyzed by a switching magnet and the neutralized beam component hit a two-dimensional position sensitive channel-plate detector. From the position information we obtained θ .

The direct proton beam, deflected in the switching magnet, was energy analyzed, with the target gas taken out, using an electrostatic parallel-plate analyzer [27]. The measured energy distribution had a width of ± 0.5 eV, which is mostly due to the resolution of the energy analyzer. The energy spread in the beam is significantly smaller. The width of the angular distribution of the direct beam was measured to be about ± 75 μ rad.

The recoiling H_2^+ and He^+ ions were extracted by a weak electric field (≈ 4.5 V/cm), directed perpendicular to the projectile beam direction, and also detected by a two-dimensional position-sensitive detector. For the smaller collision energy (25 keV)

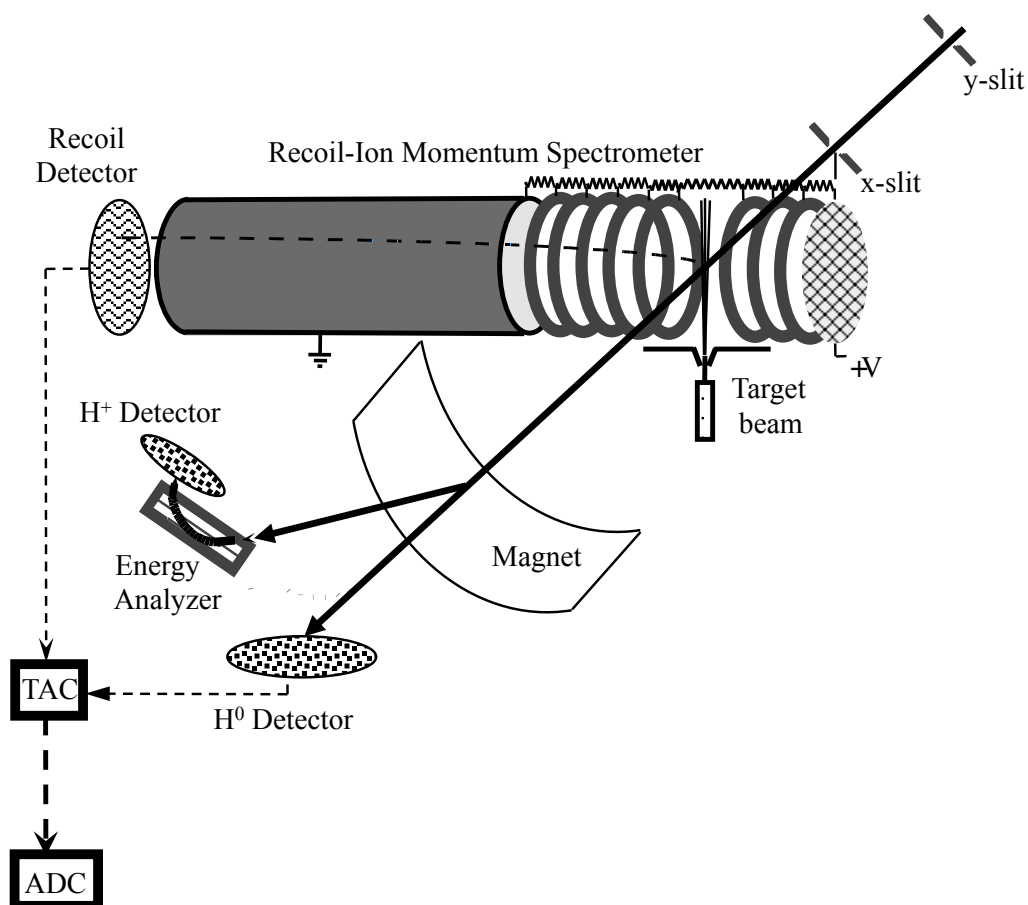


Figure 1: Schematic diagram of the experimental setup. TAC represents a time-to-amplitude converter and ADC an analog-to-digital converter.

we also obtained data for molecular proton fragments, produced in dissociative capture, extracting them with a field of about 35 V/cm. The recoil-ion detector and the neutralized projectile detector were set in coincidence. From the time-of-flight information (contained in the coincidence time spectrum) the recoil-ion momentum component in the direction of the extraction field (x-direction) was calculated and from the position information the component parallel to the projectile beam (z-direction) and the y-component were calculated. Since capture is a two-body scattering process the recoil-ion momentum is equal to the momentum transfer q from the projectile to the

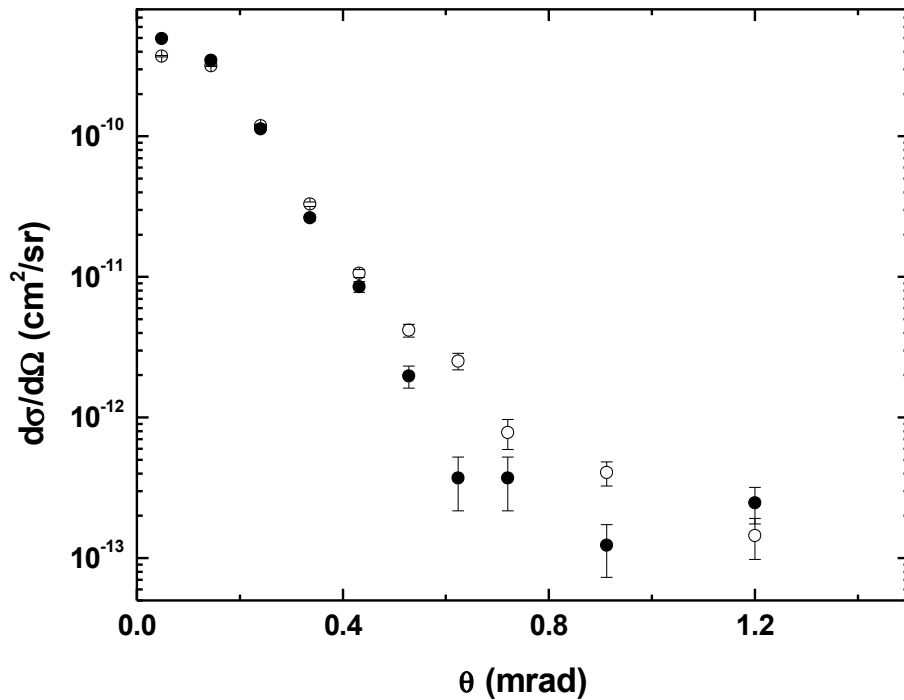


Figure 2: Differential cross sections as a function of scattering angle for nondissociative capture in 75 keV $p + H_2$ collisions. The open symbols represent the data taken at the small slit distance (i.e., for an incoherent projectile beam) and the closed symbols data taken at the large slit distance (i.e., for a coherent projectile beam).

target. For the H_2^+ and He^+ ions the momentum resolution in the y-direction (mostly due to the temperature of the target beam) was approximately ± 0.25 a.u. and in the x- and z-directions ± 0.075 a.u. In the case of the molecular proton fragments the momentum resolution was much worse (approx. ± 0.6 a.u. in all directions) due to the much larger extraction field so that here q could not be determined with sufficient accuracy from the recoil ions.

Due to the different distances of the collimating slits in the x- and y-directions the coherence length of the projectile is different in both directions. According to equation (1) in the x-direction it is $\Delta x = 0.4$ a.u. and 0.7 a.u. for a projectile energy of 75 keV and 25 keV, respectively, while for the y-direction these values are $\Delta y = 3$ a.u. and 5 a.u. so that for both energies $\Delta x < D$ and $\Delta y > D$. Therefore, by selecting projectile scattering in the x- and y-directions in the position spectrum, we obtain the differential cross sections (DCS) as a function of scattering angle for a coherent and incoherent projectile beam simultaneously in the same data run.

Results and Discussion

Since capture is kinematically a two-body scattering process the momentum analysis of one particle already constitutes a kinematically complete experiment. Therefore, for an ideal experiment, i.e. one with infinitely good resolution and no background, measuring the recoil-ion momentum in addition to the projectile momentum would not provide any additional information. However, in reality background cannot be completely avoided (and the resolution is, of course, limited). For example, the projectile position spectrum could potentially be affected by scattering from the collimating slits. If such a slit-scattered projectile subsequently undergoes a capture process with the target

this can still lead to a true coincidence. However, the scattering angle deduced from the projectile position spectrum would not be correct, while the scattering angle deduced from the recoil-ion momentum would essentially not be affected by slit scattering. Likewise, background contributions to the recoil-ion spectra, for example due to the small (but non-zero) diffusive target gas component, do not significantly affect the projectile spectra. Therefore, the over-determination of the kinematics due to the momentum-analyzed detection of both particles can be used to clean the data from such background contributions. This was achieved with the condition that θ determined from the projectiles directly and θ determined from the recoil ions must be equal within ± 0.1 mrad.

In Fig. 2 we show the DCS for non-dissociative capture in 75 keV p + H₂ collisions as a function of θ for the coherent (closed symbols) and the incoherent (open symbols) projectile beam. Once again, like in the corresponding DDCS for ionization in the same collision system [22], clear differences between the two data sets are visible. At $\theta = 0$ the coherent cross sections (DCS_{coh}) are slightly larger than the incoherent data (DCS_{inc}) before the two data sets cross around 0.2 mrad, with increasing θ the DCS_{coh} then increasingly drop below DCS_{inc} up to about $\theta = 0.8$ mrad, and both data sets seem to approach each other again with further increasing θ (although this trend at large θ is statistically not conclusive). Qualitatively, this is the same behavior as in ionization.

In analogy to classical optics the interference term IT is given by the ratio R between DCS_{coh} and DCS_{inc} [22,28], which is plotted in Fig. 3 as a function of θ . It should be noted that at $\theta = 0$ the x- and y-directions are not defined. Here, the pixels in the two-dimensional xy-position spectrum containing the events for both directions are

identical so that the ratio between the un-normalized count rates is equal to unity and does not reflect IT. Since the first data point ($\theta = 0.05$ mrad) covers the bin 0 to 0.1 mrad

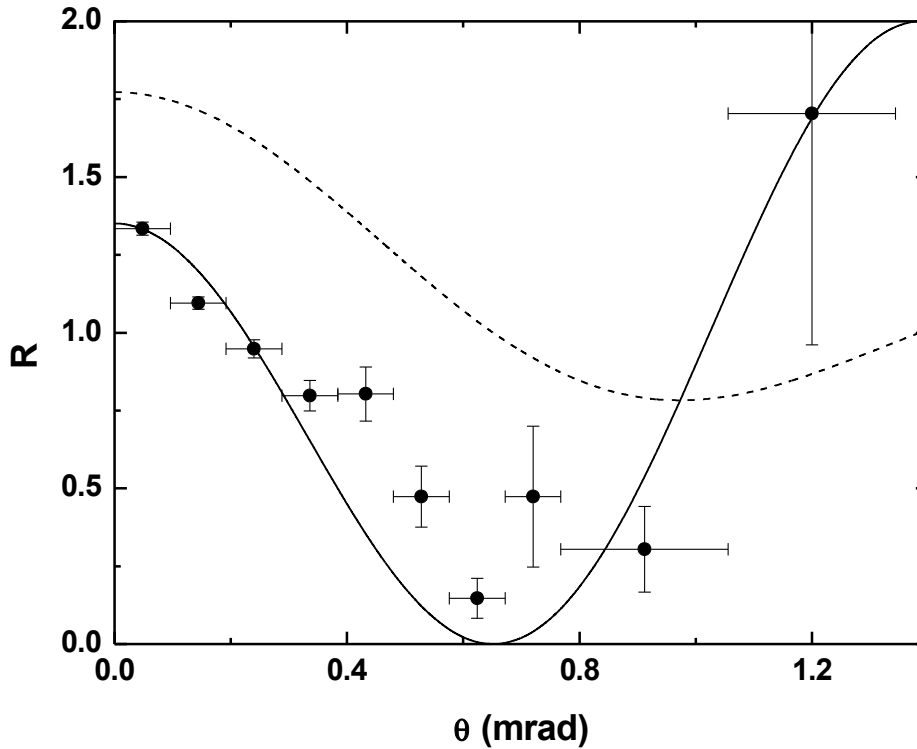


Figure 3: Differential ratios between the cross sections for a coherent and an incoherent projectile beam as a function of scattering angle for 75 keV p+H₂. Solid curve, calculation based on Eq. (2) assuming a molecular orientation along \mathbf{q} ; dashed curve, calculation based on Eq. (3).

it is partly affected. The DCS_{coh} and DCS_{inc} shown in Fig. 2 are normalized to the same total cross section [29] resulting in R differing from 1 at $\theta = 0.05$ mrad. Apart from this artifact near $\theta = 0$, once again the data look similar to the corresponding ratios for ionization.

For a fixed molecular orientation IT can be expressed as

$$\text{IT} = 1 + \cos(\mathbf{p}_{\text{rec}} \bullet \mathbf{D}) = 1 + \cos(\mathbf{q} \bullet \mathbf{D}) \quad (2)$$

In our experiment the molecular orientation was not measured and therefore IT has to be integrated over all orientations. If the angular distribution of the molecules during the capture process is isotropic this integral yields [28]

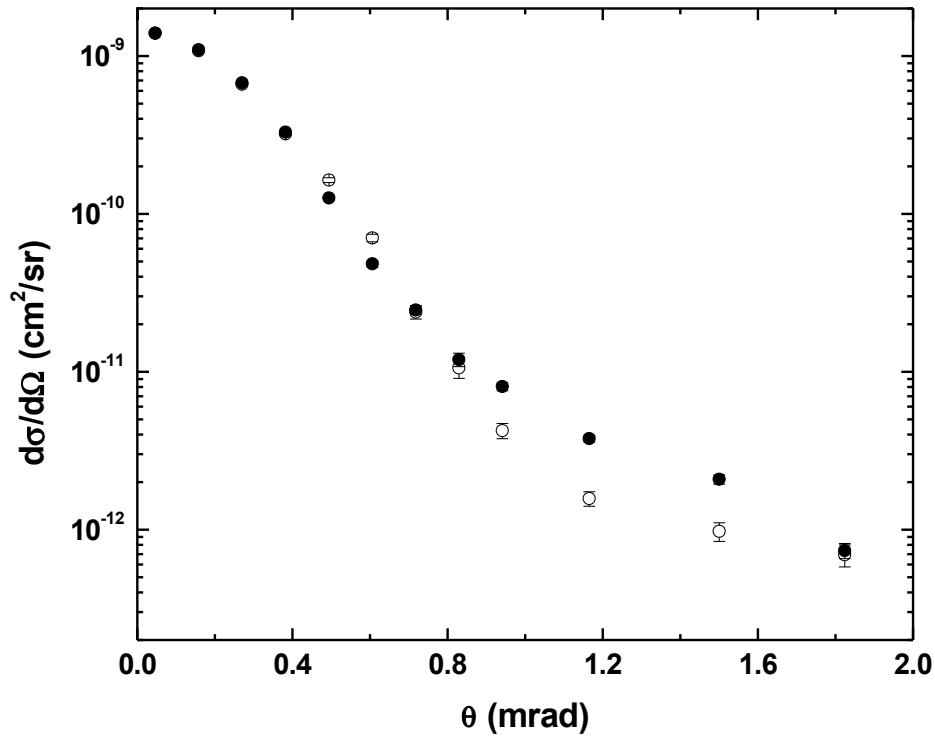


Figure 4: Same as Fig. 2 for 25 keV p+H₂.

$$IT = 1 + \sin(qD)/(qD) \quad (3)$$

On the other hand, it is not clear that all orientations are uniformly distributed. For example, in ionization of H₂ by electron impact Senftleben et al. [30] found a preference of the molecules to be oriented along q . The solid line in Fig. 3 shows IT calculated with equation (2) replacing $q \bullet D$ by qD , i.e. assuming that the molecule is always oriented along q , and the dashed curve IT calculated with equation (3). The

curves do not reach $IT = 2$ at $\theta = 0$ because q is not zero due to the θ -independent longitudinal component $q_z = \Delta E/v - v/2$ (where ΔE and v are the energy loss and the speed of the projectile). The experimental data fall, crudely speaking, in between both calculations, which is consistent with a preferential, but not exclusive, orientation along q .

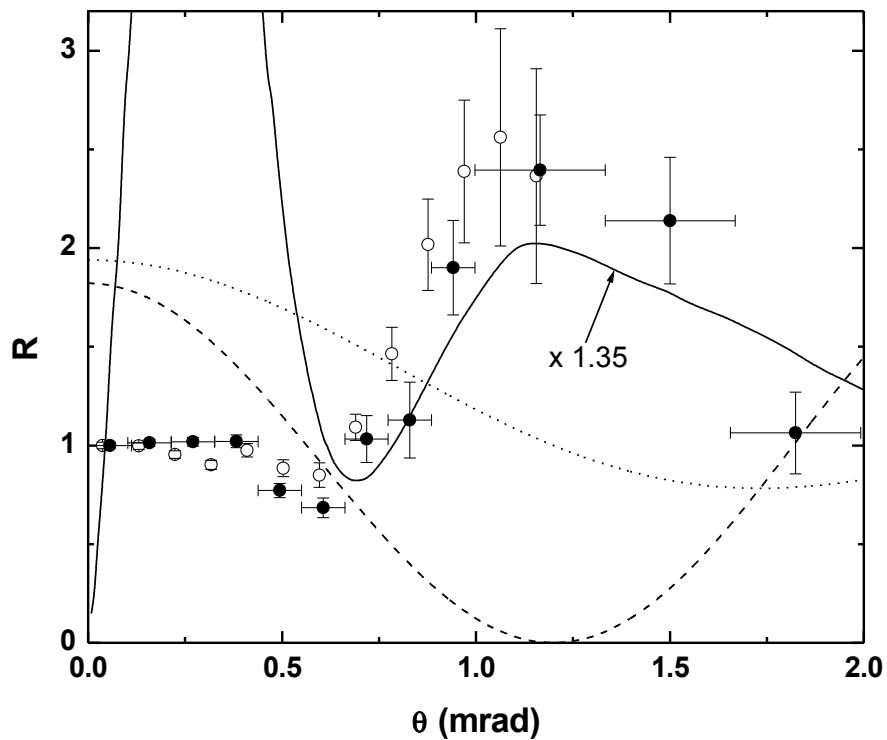


Figure 5: Same as Fig. 3 for 25 keV p+H₂ (closed symbols) and 25 keV p+He (open symbols). Dashed curve, calculation based on Eq. (2) assuming a molecular orientation along q ; dotted curve, calculation based on Eq. (3); solid curve, ratio between calculations treating the PT interaction quantum-mechanically and classically, respectively [31] (see text).

It should be noted that it is actually the component of D perpendicular to the projectile beam axis D_{\perp} which matters in the coherence requirement, which should thus read $\Delta r > D_{\perp}$. If the molecule is indeed preferentially oriented along q this means that even in the x -direction the projectile beam becomes coherent below some critical θ because q (and therefore the molecular orientation) is increasingly aligned along the beam axis with decreasing θ . However, for 75 keV this only happens at $\theta \approx 70 \mu\text{rad}$ (corresponding to a molecular orientation of about 15° relative to the beam axis) so that at most the data point at the smallest θ is affected.

In Fig. 4 the DCS_{coh} (closed symbols) and DCS_{inc} (open symbols) are shown as a function of θ for 25 keV $p + \text{H}_2$. Here too, there are some differences between both data sets. However, the comparison between DCS_{coh} and DCS_{inc} is qualitatively different from the 75 keV case. This is more apparent in the ratios R , which are plotted in Fig. 5 as a function of θ . For $\theta < 0.8 \text{ mrad}$ R is nearly constant at 1 with only a small minimum around 0.5 mrad. At large θ there is a pronounced and broad maximum near 1.2 mrad. This θ -dependence does not resemble the interference term calculated with neither eq. (2) (dashed curve in Fig. 4), assuming a molecular orientation along q , nor the one calculated with eq. (3) (dotted curve). The flat region in the experimental data, not reproduced by either calculation, could possibly be associated to some extent with the coherence requirement $\Delta r > D_{\perp}$ being satisfied even in the x -direction (small slit distance) at small θ (see above). For 25 keV this can happen already at about 0.15 mrad (where $\Delta x = D_{\perp}$, again assuming that the molecule is preferentially oriented along q) because Δx is larger than at 75 keV due to the larger DeBroglie wavelength. However, this would only explain part of the flat region, which extends to at least 0.4 mrad. More importantly, this

would not explain the maximum at large θ not reproduced by eqs. (2) or (3), which predict a minimum, rather than a maximum, in this region. The data thus seem to suggest that molecular two-center interference is either not present at 25 keV or that it is at least not the dominant interference effect.

For capture processes at small projectile energies interference structures have been observed in the calculated θ -dependence of the DCS even for atomic targets [31,32] which are thus not due to molecular two-center interference. Furthermore, it was found that this structure disappears if the PI interaction is treated classically [31]. This suggests that here too, like in the FDCS for ionization of atomic targets (see above), the interference may be due to the coherent sum of transition amplitudes with and without the PI interaction. In this case the coherence requirement is $\Delta r > \Delta b$ [26], where Δb is the difference in the impact parameter ranges, mostly contributing to a given θ , between the interfering amplitudes. In the measured DCS for 25 keV $p + H_2$ we do not observe any structures; however, the scattering angles where the extrema occur in R coincide roughly with those predicted by theory for a He target. The ratios measured for He, shown as open symbols in Fig. 5, are very similar to those for H_2 . However, the minimum near 0.5 mrad, which is rather weak for H_2 already, is even less pronounced, if present at all. The solid curve in Fig. 5 represents the ratio between the calculations of reference [31] treating the PI interaction quantum-mechanically within the eikonal approximation (dashed curve in Fig. 3a of [31]) and classically (dash-dotted curve in Fig. 3a of [31]), respectively. For a better comparison with experiment in shape the theoretical ratios were scaled up by 1.35. As far as interference between transition amplitudes with and without this interaction is concerned these calculations correspond to a coherent and

incoherent treatment. However, it should be noted that there are also differences between both calculations which are not related to the coherence. The calculation treating the PI interaction classically uses the ansatz [31]

$$d\sigma_{SC}/d\Omega(\theta) = d\sigma_{el}/d\Omega(\theta) P_{SC}(\theta) \quad (4)$$

where $d\sigma_{SC}/d\Omega(\theta)$ is the differential capture cross section, $d\sigma_{el}/d\Omega(\theta)$ the elastic

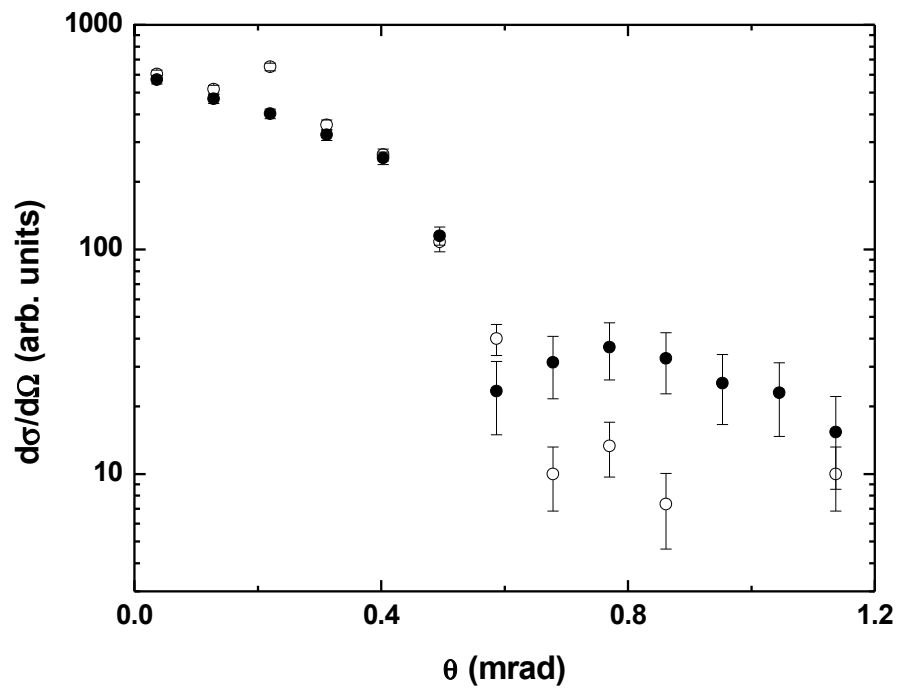


Figure 6: Same as Fig. 2 for dissociative capture in 25 keV p + H₂ .

scattering cross section, and $P_{SC}(\theta)$ the capture probability. This ansatz is not valid at θ smaller than approximately the inverse projectile momentum (≈ 0.5 mrad) [33] even if interference between the amplitudes with and without the PI interaction is unimportant. It leads to an unphysically steep increase in the cross sections (compared to both the experimental data and the calculation treating the PI interaction quantum-mechanically)

at small θ . There, the interference is not expected to be significant because the deflection of the projectile is dominated by an interaction with the target electron. The comparison

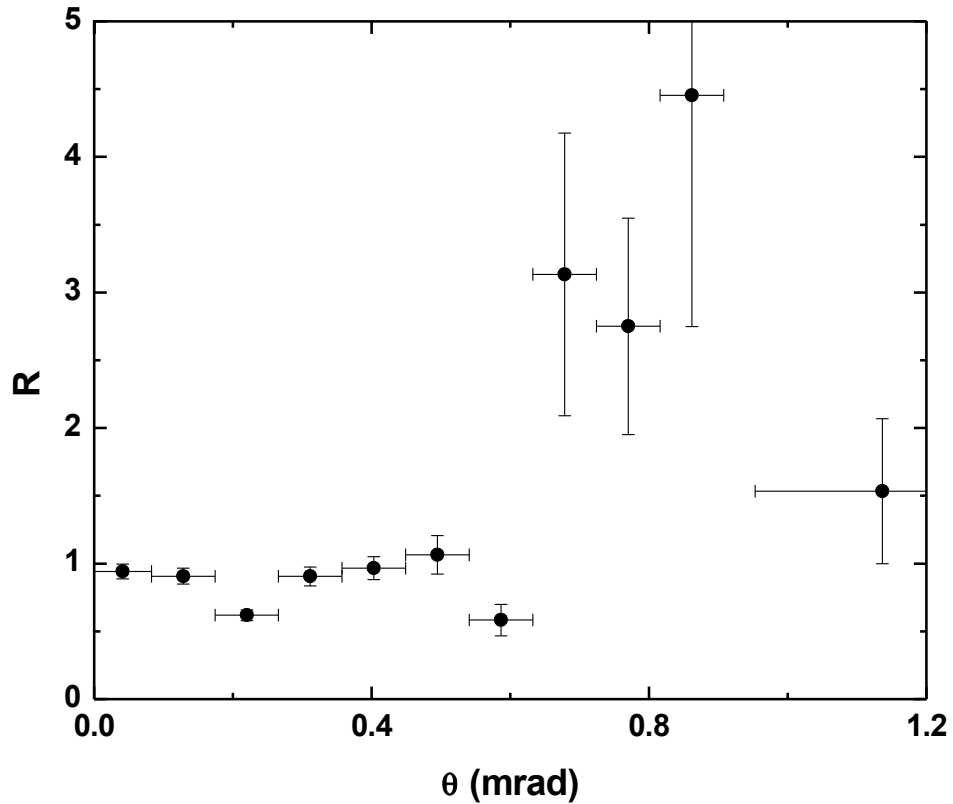


Figure 7: Same as Fig. 3 for dissociative capture in 25 keV $p + H_2$.

between the theoretical and experimental R is thus only meaningful for θ larger than approximately 0.5 mrad. In this angular range the agreement between the calculation and the measured R is surprisingly good, at least qualitatively. This shows that indeed interference effects, not immediately obvious in the absolute DCS, are actually present. On the other hand, the minimum predicted by theory around 0.7 mrad is much weaker in the experimental data (at least for the He target). This, along with the absence of

structures in the measured absolute DCS, suggests that the interference is either overestimated by theory or that the projectile beam was not fully coherent over the entire angular range even at the large slit distance.

Finally, in Fig. 6 we present DCS for dissociative capture in 25 keV $p + H_2$ collisions. Here too, the molecular orientation was not determined in the experiment. Overall, the θ -dependence of both DCS_{coh} and DCS_{inc} is significantly flatter than in the counterparts for single capture. This is expected because dissociation requires a transition of the second target electron since the ground state of H_2^+ is not dissociative. Otherwise, the comparison between DCS_{coh} and DCS_{inc} is very similar to single capture: again, the DCS are practically identical up to about 0.6 mrad. Unfortunately, at larger θ the statistical fluctuations are considerably larger than for single capture, especially in DCS_{inc} . There, the DCS are so small that in the range $\theta = 0.9$ to 1.1 mrad incoherent dissociative capture events could not even be detected. Nevertheless, even considering the large error bars, for $\theta > 0.6$ mrad DCS_{coh} is systematically larger than DCS_{inc} . In R , plotted in Fig. 7, this behavior is reflected by a θ -dependence which closely resembles the one observed for single capture from He and H_2 . In the case of single capture from He and dissociative capture from H_2 the covered θ -range is not large enough to determine the location of the maximum which for single capture from H_2 occurs at 1.2 mrad. But the rising edge appears to be slightly shifted to smaller θ for the He target and further shifted for dissociative capture.

The similarity in the structures between the He and H_2 targets and between single capture and dissociative capture observed in the θ -dependence of R suggests that in all cases they result from the same cause. The presence of this structure for an atomic target

rules out molecular two-center interference. At the same time in theoretical calculations interference effects are no longer visible if the PI interaction is treated classically [31]. This leads us to conclude that the structures are due to path interference between different impact parameters (depending on the extent to which the PI interaction is responsible for the projectile deflection) leading to the same scattering angle.

Conclusions

We have measured differential cross sections for single and dissociative capture as a function of scattering angle in collisions of 25 and 75 keV protons with He and H₂. The results confirm our previous conclusion [22] that atomic scattering cross sections can, under certain conditions, depend on the projectile coherence. For 75 keV p + H₂ we observe pronounced molecular two-center interference structures in the ratio R between the cross sections for a coherent and incoherent projectile beam similar to those reported previously for ionization in the same collision system. For 25 keV, in contrast, the structures in R are not mostly due to molecular two-center interference (although it may partly contribute), but rather they are to a large extent due to path interference between different impact parameters leading to the same scattering angle. It cannot be ruled out that the measured R for 75 keV also contain non-negligible contributions from this type of interference. Theory had predicted such structures [31,32], but in experiment they were so far not observed. Only at very small energy interference effects were found, however, in that case they are due to spatially separated quasi-molecular coupling regions [34], i.e. they are of a different nature. The present data show that path interference between different impact parameters is indeed present at larger energies (25 keV). However, it is either significantly weaker than in the calculations or the projectile beam in our

experiment was not fully coherent over the entire angular range even at the large slit distance. Furthermore, our results support the conclusion of Wang et al. [26] that the widely debated discrepancies between theory and experiment in fully differential cross sections for ionization of helium by fast C^{6+} impact [5] could be caused by such a path interference in the calculations which doesn't occur in the experimental data because there the projectile beam was incoherent.

Our studies on the role of the projectile coherence represent an important step towards resolving long-standing puzzling discrepancies between theory and experiment. Here, we discussed two examples regarding fully differential ionization cross sections for fast ion impact and differential capture cross sections for intermediate velocity proton impact. Nevertheless, further studies on this topic are called for. Regarding molecular targets fully differential measurements on ionization are underway. These experiments should reveal coherence effects much more sensitively. Furthermore, we plan to extend the studies on dissociative capture to measuring the molecular orientation. By analyzing the ratio between the coherent and incoherent data (i.e. the interference term) as a function of the molecular orientation in principle it is possible to obtain more detailed information about the coherence length. Regarding atomic targets fully differential measurements on ionization for large perturbation parameters are very important. Here, the discrepancies to theory were particularly severe and it is critical to determine whether this can be mostly blamed on the projectile coherence.

The obvious theoretical challenge is to describe an incoherent projectile beam. Presenting the projectile in terms of a wave packet with finite width is probably not feasible at present since it would require an enormous number of angular momentum

states. We propose to model the effects of an incoherent beam in a simplified manner using e.g. the second Born approximation. As discussed in this article the interference term between the 1st order amplitude and the 2nd order amplitude involving the projectile – target nucleus interaction may not be present in the experiment if the projectile beam is incoherent. An easy way to model an incoherent beam would thus be to simply omit the cross term between both amplitudes.

Acknowledgments

This research was supported by the National Science Foundation (Grant No 0969299). G.S. acknowledges support by the Fulbright Foundation. We are grateful for fruitful discussions with many friends and colleagues.

References

- [1] Dz. Belkic, I. Mancev, and J. Hanssen, *Rev. Mod. Phys.* 80, 249-314 (2008)
- [2] M. E. Rudd, Y.-K. Kim, D. H. Madison, and J. W. Gallagher, *Rev. Mod. Phys.* 57, 965 (1985)
- [3] R. Moshhammer, P.D. Fainstein, M. Schulz, W. Schmitt, H. Kollmus, R. Mann, S. Hagmann, and J. Ullrich, *Phys. Rev. Lett.* 83, 4721 (1999)
- [4] R. Moshhammer, A.N. Perumal, M. Schulz, V.D. Rodriguez, H. Kollmus, R. Mann, S. Hagmann, and J. Ullrich, *Phys. Rev. Lett* 87, 223201 (2001)
- [5] M. Schulz, R. Moshhammer, D. Fischer, H. Kollmus, D.H. Madison, S. Jones, and J. Ullrich, *Nature* 422, 48 (2003)
- [6] A. L. Harris, D. H. Madison, J. L. Peacher, M. Foster, K. Bartschat, and H. P. Saha, *Phys. Rev. A* 75, 032718 (2007)
- [7] A. B. Voitkiv and B. Najjari, *Phys. Rev. A* 79, 022709 (2009)
- [8] J. Fiol, S. Otranto, and R.E. Olson, *J. Phys. B* 39, L285 (2006)
- [9] M. Schulz, M. Dürr, B. Najjari, R. Moshhammer, J. Ullrich, *Phys. Rev. A* 76, 032712 (2007)
- [10] R.E. Olson and J. Fiol, *J. Phys. B* 36, L365 (2003)
- [11] F. Jarai-Szabo and L. Nagy, *J. Phys. B* 40 4259 (2007)
- [12] J. Colgan, M.S. Pindzola, F. Robicheaux, and M.F. Ciappina, *J.Phys. B* 44, 175205 (2011)
- [13] M. Dürr, B. Najjari, M. Schulz, A. Dorn, R. Moshhammer, A.B. Voitkiv, and J. Ullrich, *Phys. Rev. A* 75, 062708 (2007)

- [14] D.H. Madison, D. Fischer, M. Foster, M. Schulz, R. Moshhammer, S. Jones, and J. Ullrich, *Phys. Rev. Lett.* 91, 253201 (2003)
- [15] M. McGovern, C.T. Whelan, and H.R.J. Walters, *Phys. Rev. A* 82, 032702 (2010)
- [16] M. Foster, J. L. Peacher, M. Schulz, D. H. Madison, Zhangjin Chen, and H. R. J. Walters, *Phys. Rev. Lett.* 97, 093202 (2006)
- [17] A.C. Laforge, K.N. Egodapitiya, J.S. Alexander, A. Hasan, M.F. Ciappina, M.A. Khakoo, and M. Schulz, *Phys. Rev. Lett.* 103, 053201 (2009)
- [18] R.O. Barrachina and M. Zitnik, *J. Phys. B* 37, 3847 (2004)
- [19] G.R. Satchler, C.B. Fulmer, R.L. Auble, J.B. Ball, F.E. Bertrand, K.A. Erb, E.E. Gross, and D.C. Hensley, *Phys. Lett. B* 128, 147 (1983)
- [20] J.K. Swenson, J. Burgdörfer, F.W. Meyer, C.C. Havener, D.C. Gregory, and N. Stolterfoht, *Phys. Rev. Lett.* 66, 417 (1991)
- [21] J.-Y. Chesnel, A. Hajaji, R.O. Barrachina, and F. Fremont, *Phys. Rev. Lett.* 98, 100403 (2007)
- [22] K.N. Egodapitiya, S. Sharma, A. Hasan, A.C. Laforge, D.H. Madison, R. Moshhammer, and M. Schulz, *Phys. Rev. Lett.* 106, 153202 (2011)
- [23] C. Keller, J. Schmiedmayer, and A. Zeilinger, *Opt. Comm.* 179, 129 (2000)
- [24] L. Sarkadi, *Phys. Rev. A* 82, 052710 (2010)
- [25] X.Y. Ma, X. Li, S.Y. Sun, and X.F. Jia, *Europhys. Lett.* 98, 53001 (2012)
- [26] X. Wang, K. Schneider, A. LaForge, A. Kelkar, M. Grieser, R. Moshhammer, J. Ullrich, M. Schulz, and D. Fischer, submitted to *Phys. Rev. Lett.* (2012)
- [27] A.D. Gaus, W. Htwe, J.A. Brand, T.J. Gay, and M. Schulz, *Rev. Sci. Instrum.* 65, 3739 (1994)

- [28] N. Stolterfoht, B. Sulik, V. Hoffmann, B. Skogvall, J. Y. Chesnel, J. Ragnama, F. Frèmont, D. Hennecart, A. Cassimi, X. Husson, A. L. Landers, J. Tanis, M. E. Galassi, and R. D. Rivarola, *Phys. Rev. Lett.* 87, 23201 (2001)
- [29] *Atomic Data for Fusion*, C.F. Barnett (ed.), Oak Ridge National Laboratory, volume 1, A-28, Oak Ridge (1990)
- [30] A. Senftleben, T. Pflüger, X. Ren, O. Al-Hagan, B. Najjari, D. Madison, A. Dorn, and J. Ullrich, *J. Phys. B* 43, 081002 (2010)
- [31] M. Zapukhlyak, T. Kirchner, A. Hasan, B. Tooke, and M. Schulz, *Phys. Rev.* A77, 012720 (2008)
- [32] A. L. Harris, J. L. Peacher, and D. H. Madison, *Phys. Rev. A* 82, 022714 (2010)
- [33] P.T. Greenland, *J. Phys.* B14, 3707 (1981)
- [34] L.K. Johnson, R.S. Gao, R.G. Dixson, K.A. Smith, N.F. Lane, R.F. Stebbings, and M. Kimura, *Phys. Rev. A* 40, 3626 (1989)

II. Complete Momentum Balance in Ionization of H₂ by 75 keV Proton Impact for Varying Projectile Coherence

S. Sharma¹, T.P. Arthanayaka¹, A. Hasan^{1,2}, B.R. Lamichhane¹, J. Remolina¹, A. Smith¹,
and M. Schulz¹

*Dept. of Physics and LAMOR, Missouri University of Science & Technology, Rolla, MO
65409, USA*

²*Dept. of Physics, UAE University, P.O. Box 17551, Alain, Abu Dhabi, UAE*

Abstract

We report on a kinematically complete experiment on ionization of H₂ by proton impact. While a significant impact of the projectile coherence property on the scattering angle dependence of double differential cross sections (DDCS), reported earlier, is confirmed by the present data, only weak coherence effects are found in the electron and recoil-ion momentum-dependence of the DDCS. This suggests that the phase angle in the interference term is determined by the projectile momentum transfer, and not by the recoil-ion momentum. It is thus possible that the interference is not due to a two-center effect.

Introduction

The dynamics of atomic fragmentation processes have been studied extensively in order to advance our understanding of the fundamental few-body problem [e.g. 1,2]. Measurements of fully differential cross sections (FDCS) for ionization of simple target atoms or molecules by charged-particle impact have proven to be particularly important as they offer the most sensitive test of theoretical models [e.g. 1-13]. For electron impact, these studies have significantly deepened our insight of the reaction dynamics, which can be quite complex even for simple systems containing only 3 or 4 particles. Several sophisticated models were developed and over the last decade significantly improved agreement with experimental data was achieved [e.g. 1,8,14], even close to threshold, which was considered to be a particularly difficult regime.

For ion impact FDCS measurements are much more challenging due to the larger projectile mass compared to electron impact. As a result, the literature on such experiments [e.g. 2, 9-13] is not as extensive yet. Nevertheless, these studies provided some important new insights complementary to those obtained from electron impact studies. In particular, a surprisingly strong role played by the nucleus-nucleus (NN) interaction was uncovered [e.g. 2,9,15]. However, the agreement with theory was much less satisfactory than for electron impact [e.g. 16-19]. It was particularly sobering that significant discrepancies were found even for collision systems with very small perturbation parameter η (projectile charge to speed ratio) [2]. In this regime it was previously taken for granted that even the first Born approximation (FBA) would provide an adequate description of the reaction dynamics. But even state-of-the-art calculations, which diligently account for the NN interaction, did not reproduce the measured FDCS

[e.g. 16-19] and it was difficult to see where these sophisticated models could go so severely wrong.

After a decade of vivid debates we presented an experimental study which suggests that this puzzle may be resolvable by properly accounting for the coherence properties of the projectile beam realized in the experiment [20]. Double differential cross sections (DDCS) for ionization of H_2 by proton impact were measured for fixed projectile energy loss ϵ as a function of scattering angle θ . In the experiment the transverse projectile coherence length Δr was changed by placing a collimating slit of fixed width at a variable distance before the target. Since the beam was incoherent without the slit, the transverse coherence length was given by $\Delta r = L/2a \lambda$ [21], where a and L are the width of the slit and its distance to the target, respectively. The experiment was performed for two different L , one corresponding to $\Delta r > D$, resulting in a coherent beam, and the other to $\Delta r < D$, resulting in an incoherent beam, where D is the internuclear distance of the molecule. In the former case an interference structure was observed, which was absent in the latter case. The same feature was later also observed in the capture channel for the same collision system [22].

In [20] we further argued that for atomic targets interference between first- and higher-order amplitudes can be present, but that here too, they would only be observable for a coherent projectile beam. Indeed, such interference effects were found in theoretical calculations [23,24]. Since the coherence length of the massive and very fast projectile in [2] was tiny compared to the target size this could explain the puzzling discrepancies between theory and experiment. Experimental support for this interpretation was indeed obtained [25,26].

In a recent paper Feagin and Hargreaves acknowledged that our data of [20] demonstrate a projectile coherence effect, however, they argued that this should not be viewed as wave packet (de)coherence [27]. They asserted that the different DDCS measured for different collimating slit distances could be reconciled by averaging the cross sections for a fully coherent beam over the angular range within which the collimating slit is seen by the target. They further argued that if the momentum vectors of all three collision fragments were measured the scattering angle could be determined from the direct projectile-momentum measurement and from the sum momentum of the electron and the recoil ion. By selecting only events for which both angles are the same (within a small margin) the effective local collimation angle that the slit subtends at the target location should then be significantly decreased and the differences in the DDCS measured for a large and a small slit distance should be eliminated or at least strongly reduced.

In this article we report a study of ionization of H_2 by 75 keV proton impact in which all three momentum components of the scattered projectiles and of the recoiling target ions were measured. Although the ejected electron momentum was not directly measured the kinematics was nevertheless over-determined since out of the nine final-state momentum components only five are independent due to the kinematic conservation laws. We therefore did not only obtain the complete electron momentum vector, but we were also able to determine θ from the direct projectile measurement and from the momenta of the target fragments, as suggested in [27]. From the data we draw two important conclusions: a) The phase angle in the interference term does not seem to be determined by the recoil-ion momentum, as assumed previously, but rather by the

projectile momentum transfer. b) At least part of the analysis by Feagin and Hargreaves of the role of projectile coherence is not supported by our data.

Experiment

The experiment was performed at Missouri University of Science and Technology. A 75 keV proton beam was collimated with a slit of width 150 μm placed at a variable distance from the target and intersected with a cold ($T < 2$ K) neutral H_2 beam. The projectiles which were not charge-exchanged in the collision were selected by a switching magnet, decelerated to an energy of 5 keV, energy-analyzed using an

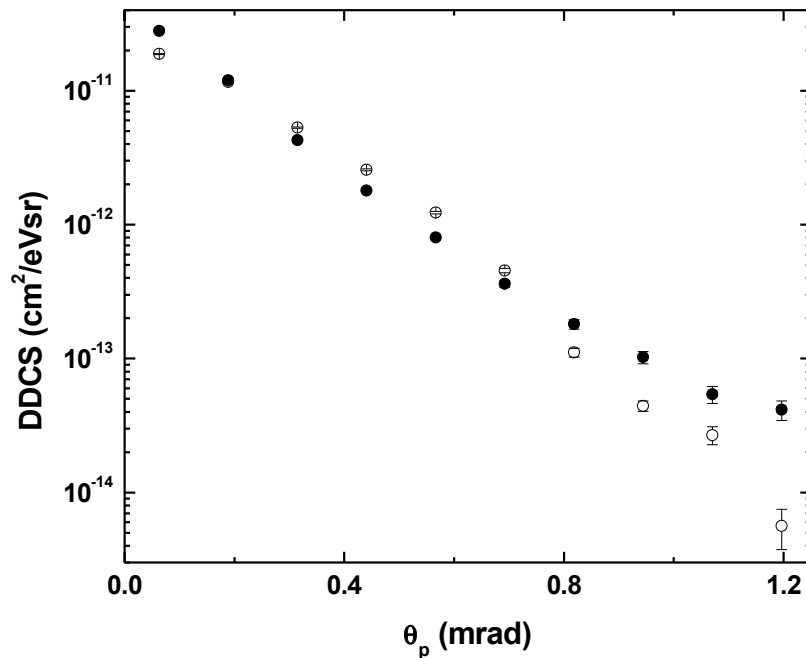


Figure 1: DDCSs for a fixed energy loss of 30 eV as a function of the projectile scattering angle θ . The closed and open data points were taken for the large and small slit distances, respectively.

electrostatic parallel-plate analyzer [28] with an energy resolution of 3 eV full width at half maximum (FWHM), and detected by a two-dimensional position sensitive multi-

channel plate (MCP) detector. The entrance and exit slits of the analyzer are narrow in the y-direction (75 μm), but long (2.5 cm) in the x-direction. Therefore, the y-

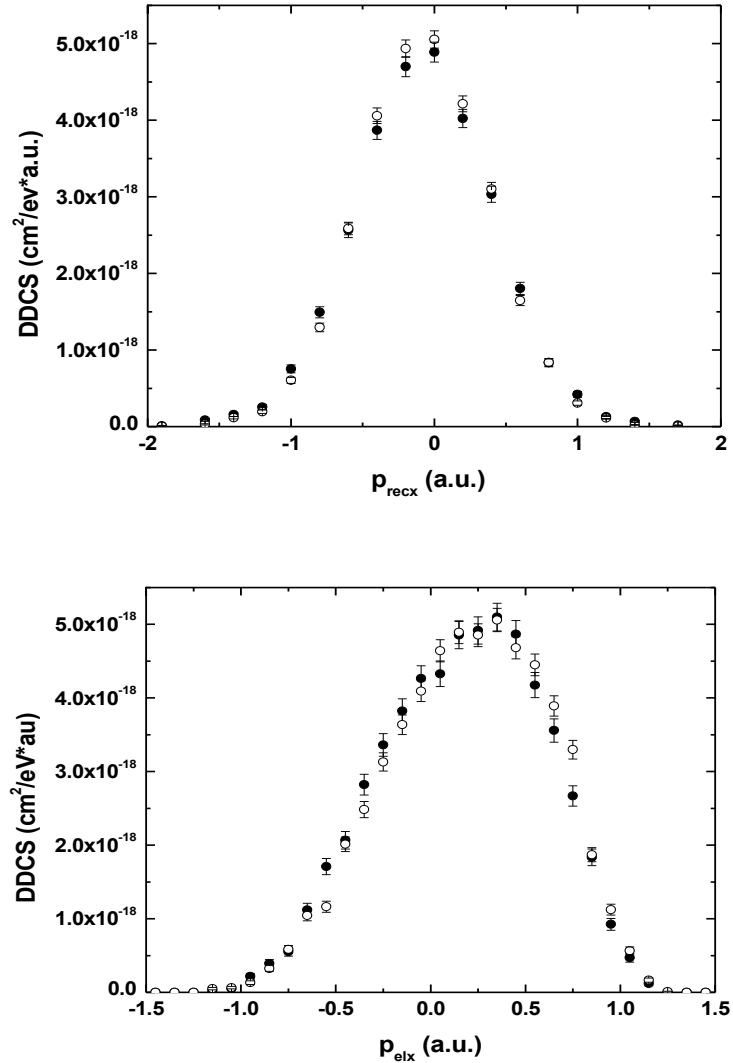


Figure 2: DDCSs for a fixed energy loss of 30 eV as a function of the x component of the recoil (top) and electron (bottom) momentum. The closed and open data points were taken for the large and small slit distances, respectively.

component of the momentum transfer q from the projectile to the target was fixed at 0 and the projectile position spectrum provided q_x and thereby the projectile scattering angle θ . The z-component is given by the projectile energy loss ε as $q_z = \varepsilon/v_p$. The

resolution in the x -, y -, and z -components of q was 0.32, 0.2, and 0.07 a.u. FWHM, respectively. The recoiling H_2^+ ions produced in the collision were extracted by a weak electric field (8 V/cm) pointing in the x -direction and momentum-analyzed by a COLTRIMS spectrometer (for a detailed description see [29]). The momentum resolution in the x -, y -, and z -direction was 0.15, 0.6, and 0.15 a.u. FWHM, respectively. The projectile and recoil-ion detectors were set in coincidence and the data recorded in event-by-event list mode. The electron momentum was deduced in the data analysis from momentum conservation. The electron energy spectrum reveals a pronounced maximum with a centroid which agrees within 0.5 eV with $\epsilon - I$, where I is the ionization potential of H_2 . A condition on this peak in the energy spectrum was used to further clean the data from any background which may have survived the coincidence time condition.

The experiment was done for two different slit distances $L = 50$ and 6.5 cm. The larger distance corresponds to a transverse coherence length of 3.3 a.u. For the smaller value the relation between Δr and the slit geometry would suggest a coherence length of 0.43 a.u.. However, it should be noted that the collimating slit can only increase, but not decrease Δr , an important point which we neglected in [20]. Without the slit Δr depends on the focus of the projectile beam and it is thus difficult to provide an accurate value. However, based on the angular profile of the beam, which provides a lower limit for the local angle under which the source of the beam is seen at the target location (and which is equivalent to L/a with collimation slit), we know that $\Delta r < 1.0$ a.u. for the small slit distance. For the larger L value $\Delta r > D$, making the beam coherent over the dimension of the molecule ($D = 1.4$ a.u.), while for the smaller L value $\Delta r < D$, corresponding to an incoherent beam.

Results and Discussion

In Fig. 1 the DDCS for $\varepsilon = 30$ eV are plotted as a function of θ . Here and in all following spectra closed circles represent data taken for large L and open circles data taken for small L. These results are consistent with those reported in [20], i.e. once again

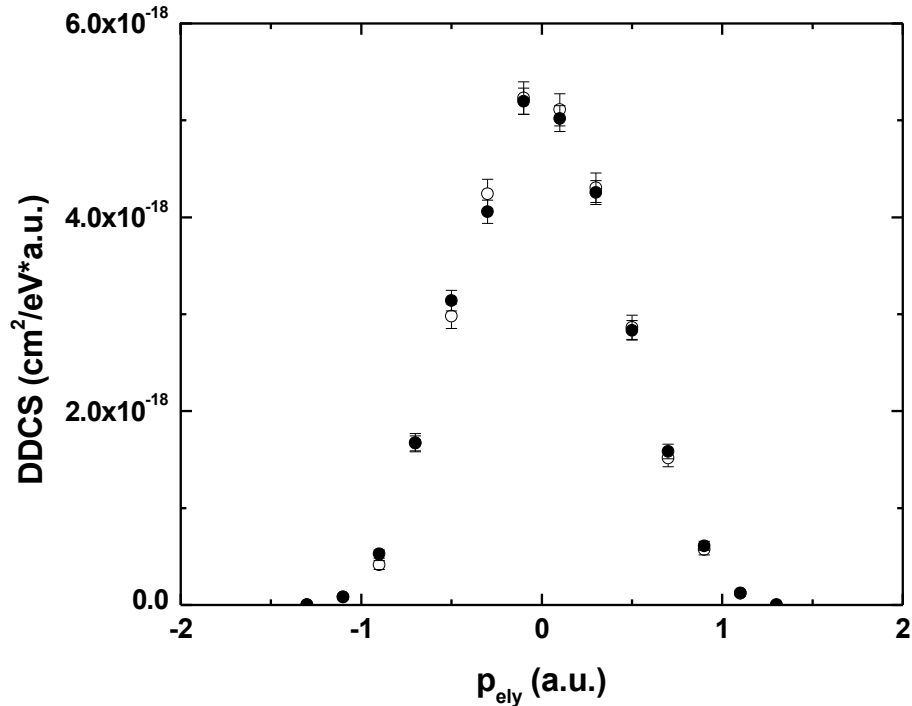


Figure 3: DDCSs for a fixed energy loss of 30 eV as a function of the y component of the electron. The closed and open data points were taken for the large and small slit distances, respectively.

we observe significant differences between the DDCS for a coherent ($DDCS_{coh}$) and an incoherent ($DDCS_{inc}$) projectile beam.

Before we analyze the projectile-differential data in more detail we first turn to the recoil-ion and electron momentum spectra. In Fig. 2 the DDCS for $\varepsilon = 30$ eV are shown as a function of the x-components (i.e. the components in the direction of the

transverse momentum transfer) of the recoil-ion momentum $p_{\text{rec}x}$ (top panel) and of the electron momentum $p_{\text{el}x}$ (bottom panel). In Fig. 3 we present the DDCS as a function of

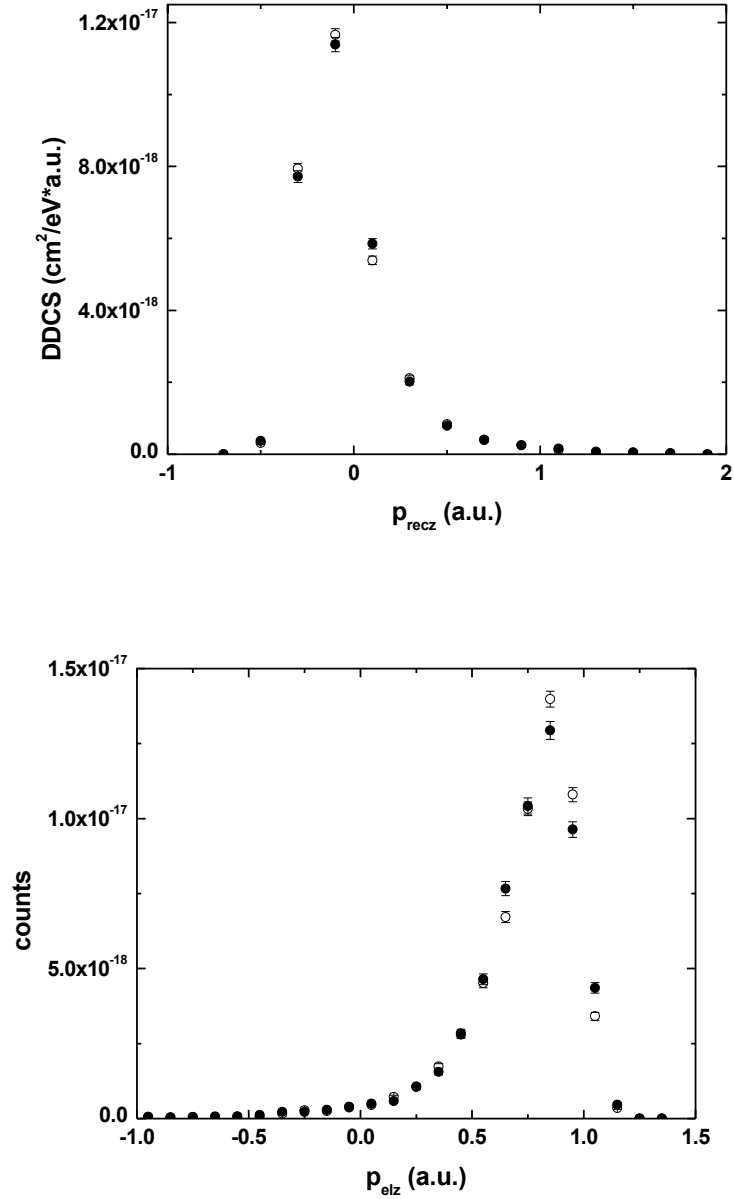


Figure 4: DDCS for a fixed energy loss of 30 eV as a function of the z component of the recoil-ion (top) and electron (bottom) momentum. The closed and open data points were taken for the large and small slit distances, respectively.

the y-component of the electron momentum p_{ely} , which (since $q_y = 0$) has the same shape as the p_{recy} dependence. Finally, in Fig. 4 the corresponding spectra are plotted for the z-components of the recoil ion and the electron momenta. All double differential data presented here were normalized to the same $d\sigma/dE_{el}$ which was used by Alexander et al.

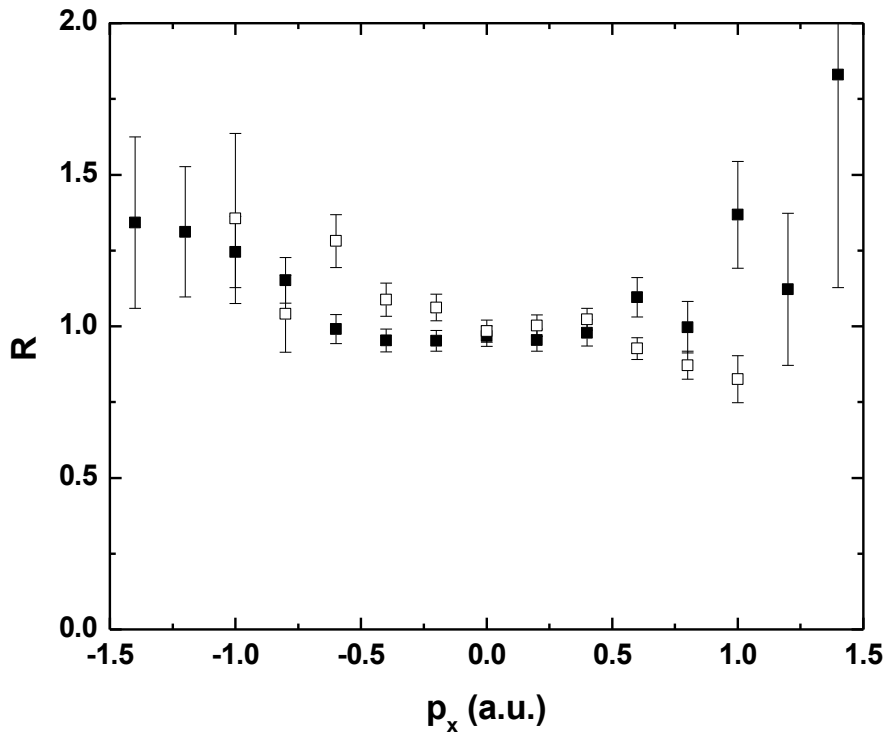


Figure 5: Ratio between the DDCSs of Fig. 2 for large and small slit distances for the electrons (open symbols) and recoil ions (closed symbols).

for normalizing their θ -dependent DDCS [30]. All electron momentum components (and $p_{recy} = -p_{ely}$) are restricted by the fixed ejected electron energy of 14.6 eV to the range -1.04 to +1.04 a.u. This also restricts the kinematically allowed range for the z-component of the recoil-ion momentum, given by $p_{recz} = q_z - p_{elz} = \epsilon/v_p - p_{elz}$, to -0.4 to

1.7 a.u. In all momentum spectra practically no counts were observed outside these kinematically allowed regions, except for small contributions due to and within the experimental resolution. Furthermore, the spectrum for p_{ely} is symmetric about 0, which is a symmetry required by the fact that neither q nor v_p have a non-zero y -component. These features observed in the data illustrate that the conditions on the coincidence time peak, on the electron energy calculated from their momentum components, and on the projectile- and recoil-ion position spectra removed essentially all of the background from the data. Both for the electrons and the recoil ions the coherent and incoherent momentum spectra for the x -component look very similar. However, a closer inspection

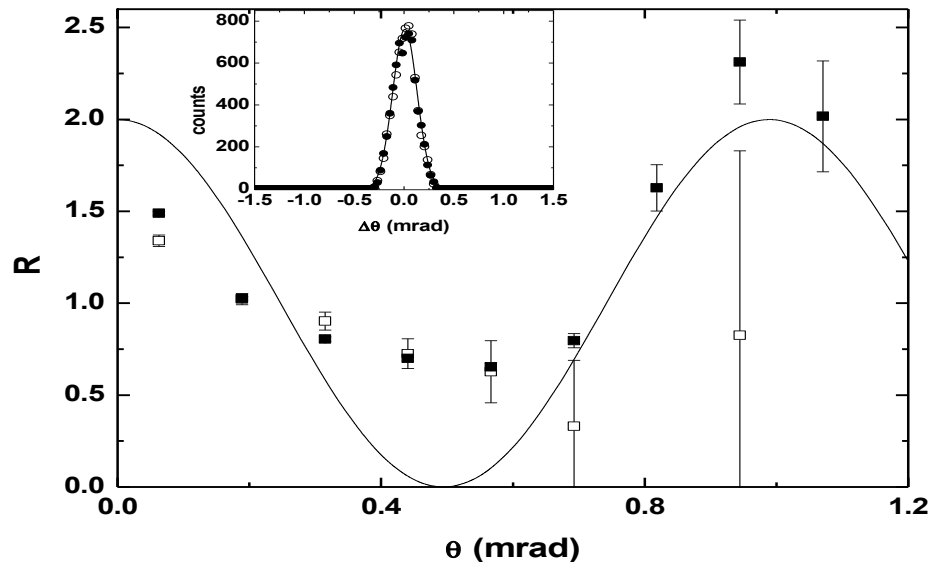


Figure 6: Ratio between the DDCSs for large and small slit distances as a function of scattering angle (closed symbols). The inset shows DDCSs as a function of the difference between the scattering angles measured directly and determined from the momenta of the target fragments. The open symbols show the ratio with the additional condition $|\Delta\theta| < 0.15$ mrad (see text). The solid line shows the interference term of the form $1 + \cos(qt \Delta b)$ with $\Delta b = 2$ a.u.

shows that for the electrons the coherent cross sections are systematically larger for $p_{\text{elx}} < 0$ and smaller for $p_{\text{elx}} > 0.5$ than the incoherent cross sections. Likewise, for the recoil ions the coherent data lie systematically above the incoherent data for $|p_{\text{recx}}| > 0.5$ a.u. and below the incoherent data for $|p_{\text{recx}}| < 0.5$ a.u. However, in both cases the differences between DDCS_{coh} and DDCS_{inc} are much smaller than in the θ -dependent cross sections.

As outlined in [20] the ratio R between DDCS_{coh} and DDCS_{inc} represents the interference term IT , which is plotted as a function of p_{elx} (open squares) and p_{recx} (closed squares) in Fig. 5. As seen already in the comparison between DDCS_{coh} and DDCS_{inc} there is only a small departure from $R = 1$. In the corresponding ratios for the DDCS as a function of the y - and z -components of the electron and recoil-ion momenta no statistically significant differences to $R = 1$ were observed at all. On the other hand if R is analyzed as a function of the sum momentum $p_{\text{elx}} + p_{\text{recx}}$, i.e. as a function of q_x , then a pronounced interference structure is observed, as we reported already in [20]. In Fig. 6 this ratio is plotted (closed squares) as a function of $\theta = \sin^{-1}(q_x/p_0)$, where p_0 is the initial projectile momentum. The structure is somewhat damped compared to the data of reference [20], which might be due to different focusing properties of the beam in the two experiments. Nevertheless, the qualitative dependence is reproduced. The phase angle in the molecular two-center interference term is believed to be determined by $p_{\text{rec}} \cdot D$ [e.g. 31,32]. The observation that the interference structure is rather weak as a function of both p_{recx} and p_{elx} , but quite pronounced in the q_x -dependence suggests that in the present data the phase angle may actually be determined by q rather than by p_{rec} . This, in turn, could be an indication that the structures we observe in $R(\theta)$ are not primarily due to this type of interference. Another possible explanation for these structures is interference

between first- and higher-order ionization amplitudes, which we dub single-center interference. Indeed, as mentioned above, such interference effects were predicted theoretically [e.g. 23,24] and fully differential data for single ionization [25] and transfer ionization [26] for collision systems with atomic targets were interpreted along this line. Unfortunately, we are not aware of any theoretical analysis providing an expression for the phase angle α leading to single-center interference. We therefore try to estimate α using a simplified semi-classical model. Suppose that b_1 and b_2 are the average impact parameters leading to the same projectile scattering angle θ by the first- and higher-order process, respectively. The classical projectile trajectories are then separated by $\Delta b = |b_1 - b_2|$. For a given θ the corresponding diffracted projectile waves reach the detector with a path difference of $d = \Delta b \sin \theta$, which results in $\alpha = (2\pi/\lambda) d = (2\pi/\lambda) \Delta b \sin \theta = q_t \Delta b$, where q_t is the transverse component of q . The interference term is then given by $IT = 1 + \cos(q_t \Delta b)$. Of course, without a rigorous treatment of the ionization process Δb cannot be determined.

However, b_1 and b_2 are surely of the order of the atomic target size so that a reasonable estimate for Δb (which can be anywhere between $|b_1| - |b_2|$ and $|b_1| + |b_2|$) is a few a.u. The solid curve in Fig. 3 shows a best fit of the interference term to the measured $R(\theta)$, which yields $\Delta b = 2$ a.u.

This discussion of a potentially important role of single-center interference should not be viewed as a firm conclusion, but rather as one possible explanation of the data which we believe is worth pursuing. However, there are alternative interpretations which should also be investigated. For example, we cannot rule out the possibility that even in two-center molecular interference α is primarily determined by q since we are not aware

of any indisputable experimental evidence to the contrary. A fully differential study of this type of interference was performed for capture in $H_2^+ + He$ collisions [33] and there the data were consistent with a phase angle given by $p_{rec} \cdot D + \pi$. However, kinematically this reaction represents a two-body scattering process so that $p_{rec} = q$. On the other hand, fully differential data for ionization of H_2 by electron impact could not be fully explained with the assumption that α is primarily determined by p_{rec} [34,35]. It is thus not clear yet whether the present data are mostly due to one- or two-center interference (or a combination of both).

Finally, we address the suggestion of Feagin and Hargreaves to plot $R(\theta)$ with the additional condition that θ directly measured and determined from the momenta of the target fragments must agree within a small margin. Although, the electron momentum was not directly measured in our experiment we can nevertheless obtain p_{elx} completely independently of q_x because measuring a total of six momentum components makes the data kinematically over-determined. Applying momentum conservation we obtain p_{ely} and p_{elz} from the directly measured $q_{y,z}$ and $p_{recy,z}$. Using energy conservation, p_{elx} is then given by $p_{elx} = \sqrt{(2E_{el} - p_{ely}^2 - p_{elz}^2)}$, where E_{el} is $\varepsilon - I$. Along with the directly measured p_{recx} this provides a second independent method of obtaining the transverse momentum transfer, which we label q_x' to distinguish it from the directly measured q_x . Finally, we compute $\Delta\theta = \sin^{-1}(q_x' - q_x)/p_o$, which is plotted for the coherent (closed symbols) and incoherent data (open symbols) in the inset of Fig. 6. With infinitely good overall resolution (including the angular spread of the incoming projectile beam) this spectrum should be a δ -function at 0. The actual spectrum is a perfectly symmetric distribution centered at $\Delta\theta = 0$ within 10 μ rad, illustrating a high accuracy in the calibration of the

measured momentum components. Using error propagation on the momentum resolutions stated in the experimental section the resolution in $\Delta\theta$ should be 0.27 mrad FWHM, which is in very good accord with the width of the actual spectrum of 0.28 mrad FWHM.

The resolution in $\Delta\theta$ does not differ noticeably for the coherent and incoherent beams. This is a first indication that the conclusion of Feagin and Hargreaves is not supported by our results. This is confirmed by $R(\theta)$ generated with the condition $|\Delta\theta| < 0.15$ mrad, which is plotted as open squares in Fig. 3. These data agree very well with $R(\theta)$ without that condition, with the possible exception of large θ . However, considering the large error bars of the data with condition in this region it is not clear whether these differences are statistically significant. Overall, the structure in $R(\theta)$ is not substantially weakened by the condition on $\Delta\theta$, contrary to the prediction of Feagin and Hargreaves [27]. We do not believe that this result entirely invalidates their analysis, which we regard as a valuable contribution. However, it does show that the differences in the cross sections measured with a coherent and an incoherent beam cannot be simply explained by experimental resolution effects.

Conclusions

In summary, we have confirmed a pronounced projectile coherence effect in the scattering angle dependence of DDCS for ionization of H_2 by proton impact. Surprisingly, in the recoil-ion momentum (and electron momentum) – dependence the coherence effect is significantly weaker. This is an indication that the phase angle in the interference term is primarily determined by q rather than by p_{rec} . The reason for this

unexpected result is presently not clear. Here, we offered two different explanations: first, the previous assumption that the phase factor in molecular two-center interference is determined by p_{rec} may be incorrect and second, the structures seen in our data may be due to a different type of interference, like e.g. interference between first- and higher-order scattering amplitudes.

We also tested the prediction by Feagin and Hargreaves that the differences between the cross sections measured for a coherent and an incoherent beam will disappear if a condition is applied that the scattering angles directly measured from the projectile and determined from the electron and recoil-ion momenta agree with each other within a small margin. Our results do not support this prediction. Rather, we find that the ratio between the cross sections for a coherent and an incoherent beam are hardly affected at all by this condition. Therefore, further analysis is called for to reconcile the theoretical work of Feagin and Hargreaves with our experimental results.

Acknowledgements

This work was supported by the National Science Foundation under grant no. PHY-0969299. We are grateful for valuable discussions with many of our friends and colleagues.

References

- [1] T.N. Rescigno, M. Baertschy, W.A. Isaacs, and C.W. McCurdy, *Science* 286, 2474 (1999)
- [2] M. Schulz, R. Moshhammer, D. Fischer, H. Kollmus, D.H. Madison, S. Jones, and J. Ullrich, *Nature* 422, 48 (2003)
- [3] H. Ehrhardt, M. Schulz, T. Tekaath, and K. Willmann, *Phys. Rev. Lett.* 22, 89 (1969)
- [4] J. Röder, H. Ehrhardt, I. Bray, D.V. Fursa, I.E. McCarthy, *J. Phys. B* 29, 2103 (1996)
- [5] A.J. Murray, M.B.J. Woolf, and F.H. Read, *J. Phys. B* 25, 3021 (1992)
- [6] M. Dürr, C. Dimopoulou, B. Najjari, A. Dorn, K. Bartschat, I. Bray, D.V. Fursa, Zhangjin Chen, D.H. Madison, and J. Ullrich, *Phys. Rev. A* 77, 032717 (2008)
- [7] A. Lahmam-Bennani, E.M. Staiacu Casagrande, and A. Naja, *J. Phys. B* 42, 235205 (2009)
- [8] X. Ren, I. Bray, D.V. Fursa, J. Colgan, M.S. Pindzola, T. Pflüger, A. Senftleben, S. Xu, A. Dorn, and J. Ullrich, *Phys. Rev. A* 83, 052711 (2011)
- [9] N.V. Maydanyuk, A. Hasan, M. Foster, B. Tooke, E. Nanni, D.H. Madison, and M. Schulz, *Phys. Rev. Lett.* 94, 243201 (2005)
- [10] M. Schulz, R. Moshhammer, A.N. Perumal, and J. Ullrich, *J. Phys. B* 35, L161 (2002)
- [11] R. Hubele, A.C. Laforge, M. Schulz, J. Goullon, X. Wang, B. Najjari, N. Ferreira, M. Grieser, V.L.B. de Jesus, R. Moshhammer, K. Schneider, A.B. Voitkiv, and D. Fischer, *Phys. Rev. Lett.* 110, 133201 (2013)
- [12] M. Schulz, B. Najjari, A.B. Voitkiv, K. Schneider, X. Wang, A.C. Laforge, R. Hubele, J. Goullon, N. Ferreira, A. Kelkar, M. Grieser, R. Moshhammer, J. Ullrich, and D. Fischer, *Phys. Rev. A* 88, 022704 (2013)

- [13] M. Schulz and D.H. Madison, *International Journal of Modern Physics A* 21, 3649 (2006)
- [14] Z. Chen, D.H. Madison, and K. Bartschat, *J. Phys. B* 40, 2333 (2007)
- [15] M. Schulz, R. Moshhammer, D. Fischer, and J. Ullrich, *J. Phys. B* 36, L311 (2003)
- [16] D. Madison, M. Schulz, S. Jones, M. Foster, R. Moshhammer, and J. Ullrich, *J. Phys. B* 35, 3297 (2002)
- [17] K.A. Kouzakov, S.A. Zaytsev, Yu. V. Popov, and M. Takahashi, *Phys. Rev. A* 86, 032710 (2012)
- [18] M. McGovern, C.T. Whelan, and H.R.J. Walters, *Phys. Rev. A* 82, 032702 (2010)
- [19] M. McGovern, D. Assafrão, J.R. Mohallem, C.T. Whelan, and H.R.J. Walters *Phys. Rev. A* 81, 042704 (2010)
- [20] K.N. Egodapitiya, S. Sharma, A. Hasan, A.C. Laforge, D.H. Madison, R. Moshhammer, and M. Schulz, *Phys. Rev. Lett.* 106, 153202 (2011)
- [21] C. Keller, J. Schmiedmayer, and A. Zeilinger, *Opt. Comm.* 179, 129 (2000)
- [22] S. Sharma, A. Hasan, K.N. Egodapitiya, T. P. Arthanayaka, and M. Schulz, *Phys. Rev. A* 86, 022706 (2012)
- [23] X.Y. Ma, X. Li , S.Y. Sun, and X.F. Jia, *Europhys. Lett.* 98, 53001 (2012)
- [24] A.B. Voitkiv, B. Najjari, and J. Ullrich, *J. Phys. B* 36, 2591 (2003)
- [25] X. Wang, K. Schneider, A. LaForge, A. Kelkar, M. Grieser, R. Moshhammer, J. Ullrich, M. Schulz, and D. Fischer, *J. Phys. B* 45, 211001 (2012)
- [26] K. Schneider, M. Schulz, X. Wang, A. Kelkar, M. Grieser, C. Krantz, J. Ullrich, R. Moshhammer, and D. Fischer, *Phys. Rev. Lett.* 110, 113201 (2013)

- [27] J.M. Feagin and L. Hargreaves, Phys. Rev. A 88, 032705 (2013)
- [28] A.D. Gaus, W. Htwe, J.A. Brand, T.J. Gay, and M. Schulz, Rev. Sci. Instrum. 65, 3739 (1994)
- [29] M. Schulz, A. Hasan, N.V. Maydanyuk, M. Foster, B. Tooke, and D.H. Madison, Phys. Rev. A 73, 062704 (2006)
- [30] J.S. Alexander, A.C. Laforge, A. Hasan, Z.S. Machavariani, M.F. Ciappina, R.D. Rivarola, D.H. Madison, and M. Schulz, Phys. Rev. A 78, 060701(R) (2008)
- [31] N. Stolterfoht, B. Sulik, V. Hoffmann, B. Skogvall, J. Y. Chesnel, J. Ragnama, F. Frémont, D. Hennecart, A. Cassimi, X. Husson, A. L. Landers, J. Tanis, M. E. Galassi, and R. D. Rivarola, Phys. Rev. Lett. 87, 23201 (2001)
- [32] S.E. Corchs, R.D. Rivarola, J.H. McGuire, and Y.D. Wang, Phys. Scr. 50, 469 (1994)
- [33] L.Ph.H. Schmidt, S. Schössler, F. Afaneh, M. Schöffler, K.E. Stiebing, H. Schmidt-Böcking, and R. Dörner, Phys. Rev. Lett. 101, 173202 (2008)
- [34] Z.N. Ozer, H. Chaluvadi, M. Ulu, M. Dogan, B. Aktas, and D.H. Madison, Phys. Rev. A 87, 042704 (2013)
- [35] A. Senftleben, T. Pflüger, X. Ren, O. Al-Hagan, B. Najjari, D.H. Madison, A. Dorn and J. Ullrich, J. Phys. B 43 081002 (2010)

III. Fully Differential Study of Interference in Ionization of H₂ by Proton Impact

S. Sharma¹, T.P. Arthanayaka¹, A. Hasan^{1,2}, B.R. Lamichhane¹, J. Remolina¹, A. Smith¹,
and M. Schulz¹

¹Dept. of Physics and LAMOR, Missouri University of Science & Technology, Rolla,
MO 65409

²Dept. of Physics, UAE University, P.O. Box 15551, Al Ain, Abu Dhabi, UAE

Abstract

We have measured fully differential cross sections for ionization of H₂ by 75 keV proton impact. The coherence length of the projectile beam was varied by changing the distance between a collimating slit and the target. Pronounced coherence effects, observed earlier in double differential cross sections, were confirmed. A surprising result is that the phase angle in the interference term is primarily determined by the momentum transfer, and only to a lesser extent by the recoil-ion momentum.

Introduction

Over the last 10 to 15 years kinematically complete experiments (i.e. experiments which determine the momentum vectors of all particles in the system under investigation) revealed that the description of the spatial and temporal evolution of systems as simple as two positively charged ions interacting with an electron represent a formidable theoretical challenge [e.g. 1-12]. The basic problem is that the Schrodinger equation is not analytically solvable for more than two mutually interacting particles, even when the underlying forces are precisely known. This dilemma is known as the few-body problem (FBP). As a result, theory has to resort to approximations and numeric approaches. Even for a simple system containing only three particles the theoretical codes can become very complex and realistically modelling an exact solution is only possible with the aide of very large computational efforts and resources. For ionization of atoms and molecules by ion impact calculations are particularly challenging because of the large projectile mass, which means that an enormous number of angular momentum states of the incoming and outgoing projectiles has to be accounted for. Indeed, qualitative discrepancies between calculated and measured fully differential cross sections (FDCS) for ionization of helium were observed even in the case of very fast projectiles [e.g. 1,6,12], which were thought to represent a relatively “easy” case. For smaller projectile speeds and especially for larger charge states the discrepancies become even larger [e.g. 3,4,9].

After a decade of vivid debates a possible explanation, based on the projectile coherence properties, for some of these surprising discrepancies was offered [13]. Earlier, interference structures in the ejected electron spectra [e.g. 14,15], in the scattering angle dependence of double differential cross sections [16], and in the molecular orientation dependent cross section for ionization of or capture from molecular

hydrogen [17] were reported. This interference was interpreted as being due to indistinguishable electron ejection [14,15] or diffraction of the projectile wave [16] from the two atomic centers in the molecule. However, later it was argued that interference effects in the scattering angle dependence are only present if the projectile beam is coherent, i.e. if the coherence length is larger than the dimension of the diffracting object [13]. It was further argued that in ionization of atomic targets different types of interference (e.g. between first- and higher-order transition amplitudes) can be present, but that here, too, the coherence requirements must be satisfied. While fully quantum-mechanical models assumed a fully coherent beam, the transverse coherence length realized in the experiment reported in [1] (and in many other fully differential measurements) was much smaller than the size of the target atom. Later, this explanation for the discrepancies between experiment and theory was supported by FDCS measured for a projectile beam with a much larger transverse coherence length [18], for which the discrepancies were significantly reduced.

The findings on the role of projectile coherence reported in [13] have led to further intense discussions. Feagin and Hargreaves acknowledged that the data presented in [13] demonstrate a projectile coherence effect, but they argued that this should not be seen as a wave packet coherence effect [19]. Instead, they asserted that the effects observed in [13] are due to an incoherent superposition of an ensemble of projectiles originating from an extended source. In a recent experimental study we tested their theoretical analysis and found that it was not fully supported by our data [20]. There, we analyzed the angular resolution of the detected projectiles and experimentally determined that the resolutions for the supposedly coherent and incoherent beams did not differ

significantly. In contrast, Feagin and Hargreaves had to assume that the resolution for the incoherent beam had to be substantially worse (nearly an order of magnitude) in order to reproduce the experimental data. While the results of [20] did not disprove the assertion in [19] that the coherence effect reported in [13] should not be viewed as a wavepacket coherence effect, they did demonstrate that it is not merely due to an experimental resolution effect either.

In [20] we also found indications that the phase angle entering in the interference term is not primarily determined by the recoil-ion momentum, which was believed to be the case for two-center molecular interference, but rather by the transverse component of the momentum transfer \mathbf{q} from the projectile to the target. These observations, as well as the theoretical analysis of [19], show that further investigations of the role of the projectile coherence and interference effects in ionization of molecular hydrogen are needed. In this article we report the first fully differential study of interference effects in target ionization by ion impact. The data support our previous interpretation that the projectile coherence properties generally can have a significant impact on the collision cross sections. However, they do not settle the question whether this can be viewed as a wave packet coherence effect as discussed in [19]. Furthermore, the present data confirm that the phase angle in the interference term is primarily determined by the transverse momentum transfer.

Experimental set-up

The experiment was performed at the projectile- and recoil-ion momentum spectrometer facility at *Missouri S & T*. A sketch of the set-up is shown in Fig. 1. A proton beam was generated with a hot cathode ion source (where the cathode is a

filament) and extracted through an anode aperture with a diameter of 0.5 mm. The beam was focused by an electrostatic lens and collimated by a second aperture 1.5 mm in diameter and located about 45 cm from the lens.

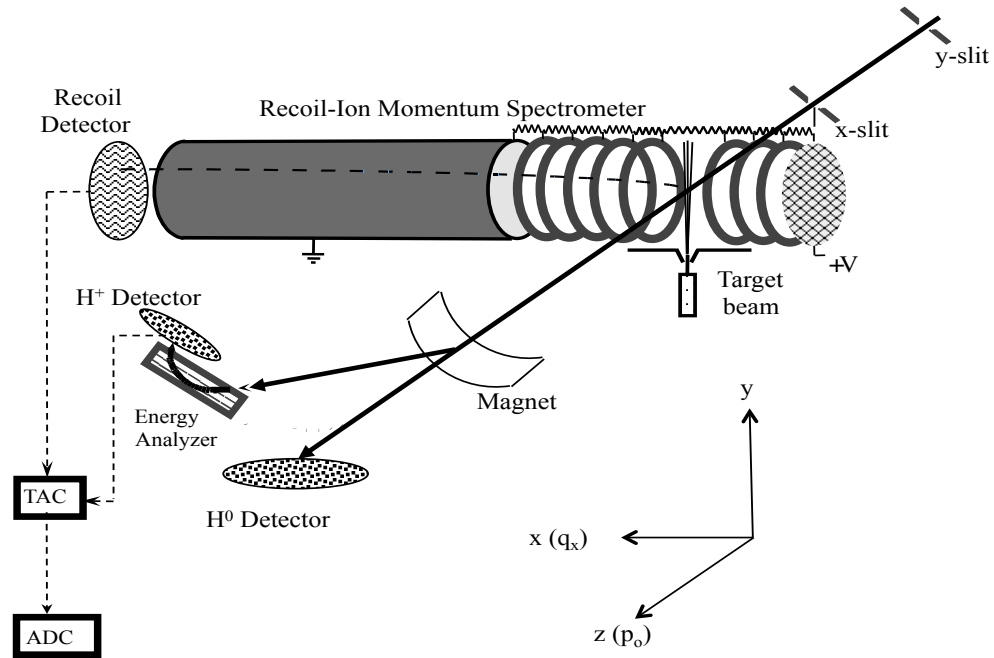


Figure 1: Schematic diagram of the experimental set-up.

After acceleration to an energy of 75 keV the proton beam was further collimated in the x-direction with a vertical slit of width $150\ \mu\text{m}$ located approximately 150 cm from the aperture and placed at a variable distance from the target. A second slit, oriented horizontally, used to collimate the beam in the y-direction (also with a width of $150\ \mu\text{m}$), was kept at a fixed distance from the target (a few mm from the large-distance location of the x-slit). The collimated proton beam was then intersected with a very cold ($T \cong 1\text{-}2\ \text{K}$) neutral H_2 beam generated by a supersonic gas jet. The transverse coherence length Δr of the projectiles was varied by placing the collimating slit at two different distances ($L_1 =$

6.5 cm, $L_2 = 50$ cm) from the target. Without the slit Δr at the target would be less than 1 a.u., which, since the slit can only increase, but not decrease Δr , coincides with Δr with the slit placed at L_2 , while L_1 yields $\Delta r = 3.3$ a.u.

The projectiles which did not charge-exchange in the collision were selected by a switching magnet, decelerated by 70 keV, and energy-analyzed by an electrostatic parallel-plate analyzer [21]. The beam component which suffered an energy loss of 30 eV was detected by a two-dimensional position sensitive channel-plate detector. From the position information in the x-direction (defined by the orientation of the analyzer entrance and exit slits) the x-component of \mathbf{q} could be determined. Because of the very narrow width of the analyzer slits (75 μm) the y-component of \mathbf{q} was fixed at 0 for all detected projectiles. The z-component (pointing in the projectile beam direction) of \mathbf{q} is given by $q_z = \epsilon/v_p$, where ϵ and v_p are the energy loss and the speed of the projectiles. The resolution in the x-, y-, and z-components of \mathbf{q} was 0.32, 0.2, and 0.07 a.u. full width at half maximum (FWHM), respectively.

The H_2^+ ions produced in the collisions were extracted by a weak electric field of 8 V/cm and then drifted in a field-free region, twice as long as the extraction region, before hitting another two-dimensional position-sensitive channel-plate detector. From the position information the y- and z-components of the recoil-ion momentum could be determined. The two detectors were set in coincidence and the coincidence time is, apart from a constant offset, equal to the time of flight of the recoil ions from the collision region to the detector. From it, the x-component of the recoil-ion momentum can be determined. The momentum resolution in the x-, y-, and z-direction was 0.15, 0.5, and

0.15 a.u. FWHM, respectively. Finally, the electron momentum was deduced from momentum conservation by $\mathbf{p}_{\text{el}} = \mathbf{q} - \mathbf{p}_{\text{rec}}$.

Results and discussion

The FDCS can be presented in many different ways. One common method, originally introduced to present FDCS for ionization by electron impact (for a review see e.g. [22]) and later adopted for ion impact (for a review see e.g. [23]) is to fix the magnitude of \mathbf{q} (or equivalently the projectile scattering angle) and the ejected electron energy and to plot the FDCS as a function of the azimuthal and polar electron emission angles φ_{el} and θ_{el} . Here, θ_{el} is measured relative to the projectile beam axis and φ_{el} relative to the transverse component of \mathbf{q} (which in our coordinate system is equal to its x-component q_x). An example of such three-dimensional fully differential angular distributions of the ejected electrons is shown in Fig. 2 for $q = 0.9$ a.u..

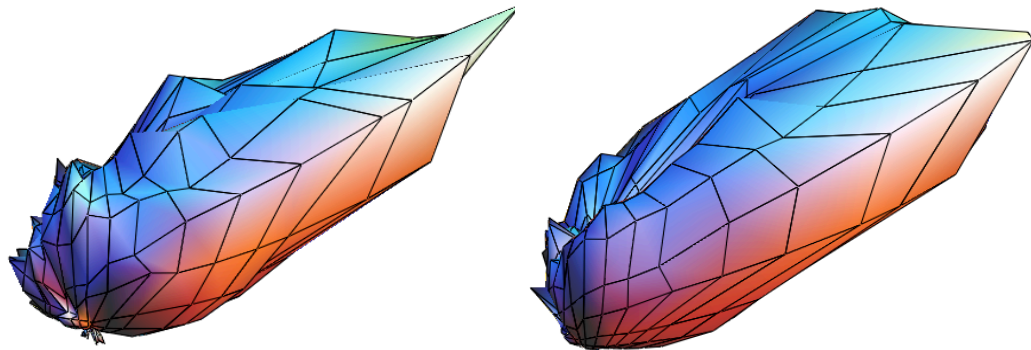


Figure 2: Fully differential, three-dimensional angular distribution of the ejected electrons taken for the large (left panel) and small (right panel) slit distance and for a momentum transfer of 0.9 a.u.

The data in the left panel were taken for the large slit distance and those in the right panel for the small slit distance. As far as the shape of the angular dependence is concerned, only relatively small differences between these two data sets were observed. These differences occur mostly outside the scattering plane, spanned by the initial and final projectile momenta, where the FDCS maximize.

The similarity between the spectra of Fig. 2 for small and large slit distances is consistent with the conclusion reported in [20] that the phase angle in the interference term is not primarily determined by the recoil momentum, but rather by q_x . Since q_x is fixed in the data of Fig. 2 the angular shape of the FDCS should then not be affected much by the interference term. Therefore, in order to extract detailed information about the phase angle from the data it is advantageous to find a representation of the FDCS in which q_x changes with φ_{el} and/or θ_{el} . One possibility is to generate the fully differential electron angular distribution for a fixed x-component of \mathbf{p}_{rec} rather than for fixed q (which is equivalent to fixing q_x because $q_y = 0$ and q_z is constant for a fixed electron energy). In such a presentation each set of φ_{el} and θ_{el} corresponds to a different q_x according to

$$q_x = p_{recx} + p_{el} \sin \varphi_{el} \sin \theta_{el} \quad (1)$$

In Fig. 3 the FDCS for p_{recx} fixed at -0.2 a.u. (left panel) and +0.2 a.u. (right panel) are shown for electrons ejected into the scattering plane as a function of θ_{el} (i.e. φ_{el} is fixed at 90°). Here, we are using a non-conventional coordinate system in which θ_{el} varies between 0 and 360° and φ_{el} between 0 and 180° . For the angular range 0 to 180° the x-component of the electron momentum is parallel to q_x . It should be noted that the positive x-direction is determined by q_x , i.e. by choice of the coordinate system $q_x < 0$ is

not possible. Therefore, only the angular ranges 11° to 169° and -11° to 191° are possible for $p_{\text{reco}} = -0.2$ a.u. and $p_{\text{reco}} = 0.2$ a.u., respectively; outside these regions $q_x < 0$.

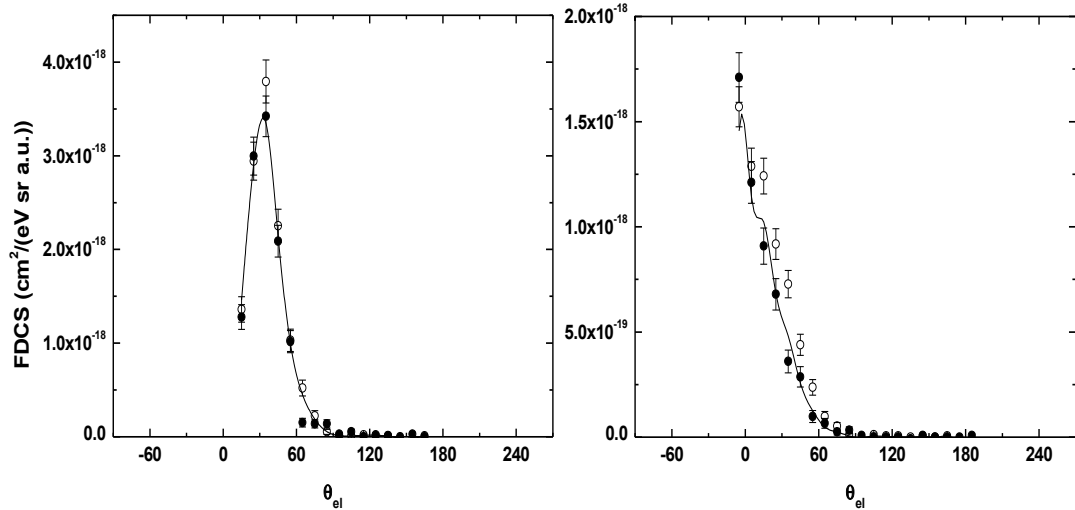


Figure 3: Fully differential cross sections for electrons ejected into the scattering plane as a function of the polar emission angle. The x-component of the recoil-ion momentum was fixed at -0.2 a.u. (left panel) and $+0.2$ a.u. (right panel). The closed (open) symbols represent the data taken for the large (small) slit distance. The solid lines represent the product of the incoherent data with an interference term of the form $1 + \alpha \cos(q_x D)$ (see text for details).

The data represented by the closed symbols were taken for the large slit distance and those represented by the open symbols for the small slit distance. In the case of $p_{\text{reco}} = -0.2$ a.u. no significant differences in the angular dependence of both data sets is found. However, for $p_{\text{reco}} = 0.2$ a.u. and in the angular range $\theta_{\text{el}} \cong 15^\circ$ to 75° the FDCS for the coherent beam are systematically smaller than for the incoherent beam.

One disadvantage of analyzing interference effects in the FDCS for electrons ejected into the scattering plane is that here the angular electron distribution is sharply peaked, especially for $p_{\text{reco}} = -0.2$ a.u. As a result, the variation of the phase angle in the

interference term is limited to a narrow range for which data can be collected with sufficient statistics. In order to avoid this problem we also analyzed the azimuthal angular dependence of the FDCS for fixed polar angles of the ejected electrons. Here, we switch back to conventional spherical coordinates in which θ_{el} runs from 0 to 180° and φ_{el} from 0 to 360° . Since the FDCS are very small for $\theta_{el} > 60^\circ$ we present the φ_{el} -dependence of the FDCS for (from top to bottom) $\theta_{el} = 15^\circ, 35^\circ,$ and 55° and for $p_{recx} = -0.2$ a.u. (left panels) and $p_{recx} = 0.2$ a.u. (right panels) in Fig. 4. Here too, as in Fig. 3, the angular ranges for which no data are shown are kinematically not allowed because $q_x < 0$. In this representation of the data the structures in the FDCS are much broader than in the θ_{el} -dependence for electrons ejected into the scattering plane. Once again, for $p_{recx} = -0.2$ a.u. only small, but for $p_{recx} = 0.2$ a.u. significant differences between the FDCS for the coherent and incoherent beams can be seen.

If the projectile beam is coherent for large L and incoherent for small L the ratio R between the cross sections for these slit distances represents the interference term, as outlined in [13]. In the following we analyze to what extent the measured ratios are consistent with the FDCS being affected by interference effects. R is plotted as a function of φ_{el} in Fig. 5 for the same kinematic settings (and in the same order) as for the FDCS of Fig. 4. The horizontal error bars show the angular resolution of the ejected electrons, which was estimated using a Monte Carlo simulation [24].

Two trends are seen in Fig. 5: first, the interference structure is more pronounced for positive than for negative p_{recx} , and second the interference structure becomes more pronounced with increasing θ_{el} . Since for fixed values of θ_{el} , p_{recx} , and of the electron energy φ_{el} unambiguously determines q_x the variation of the interference term with φ_{el}

implies that the phase angle depends on q_x . In ref. [20] we showed that within a simple, geometric model the position of the interference extrema in the measured scattering angle dependence of the double differential cross section ratios between the coherent and

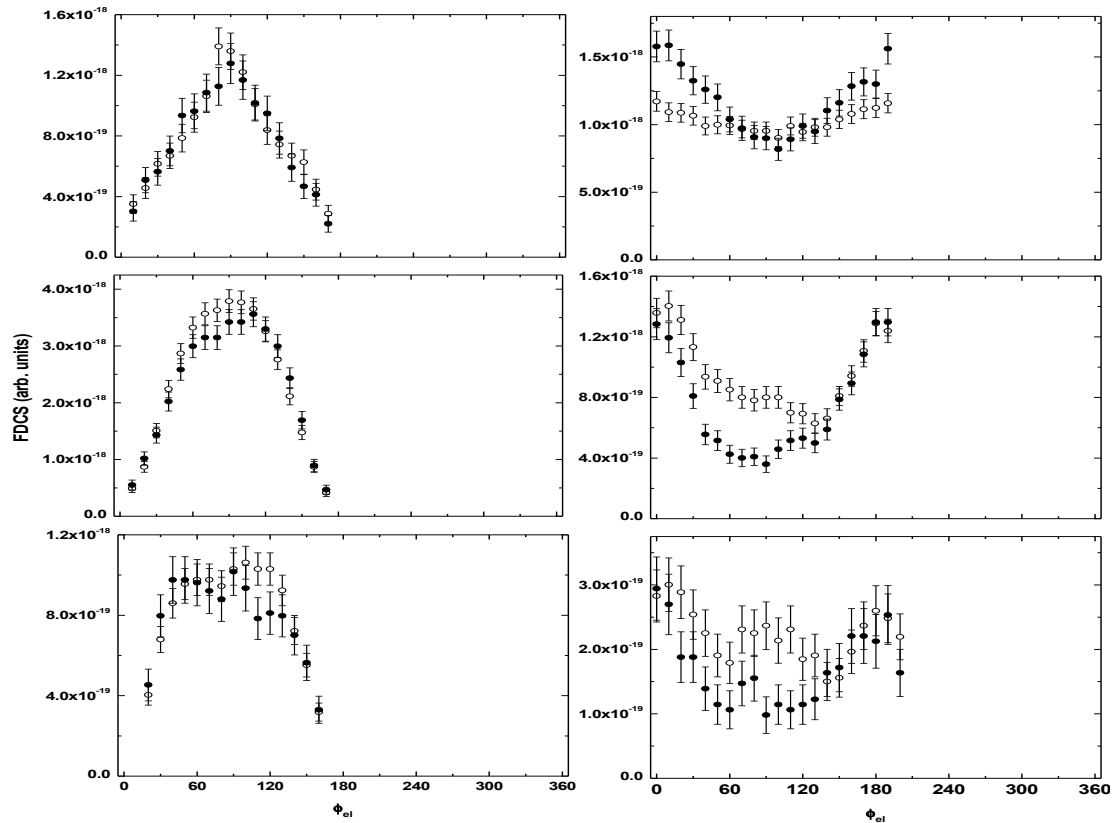


Figure 4: Fully differential cross sections as a function of the azimuthal electron ejection angle for fixed polar angles of 15° (top panels), 35° (center panels), and 55° (bottom panels). The x-component of the recoil-ion momentum was fixed at -0.2 a.u. (left panels) and $+0.2$ a.u. (right panels). Symbols as in Fig. 3.

incoherent beams can be fitted quite well by an interference term of the form $I = 1 + \alpha \cos(q_x D)$ with $D = 2$ a.u. and $\alpha = 0.5$. This relation, with q_x determined from equation (1), is shown in Fig. 5 as the solid curves. The constant α in I accounts for the “damping” of the interference due to incomplete coherence even for the large slit distance

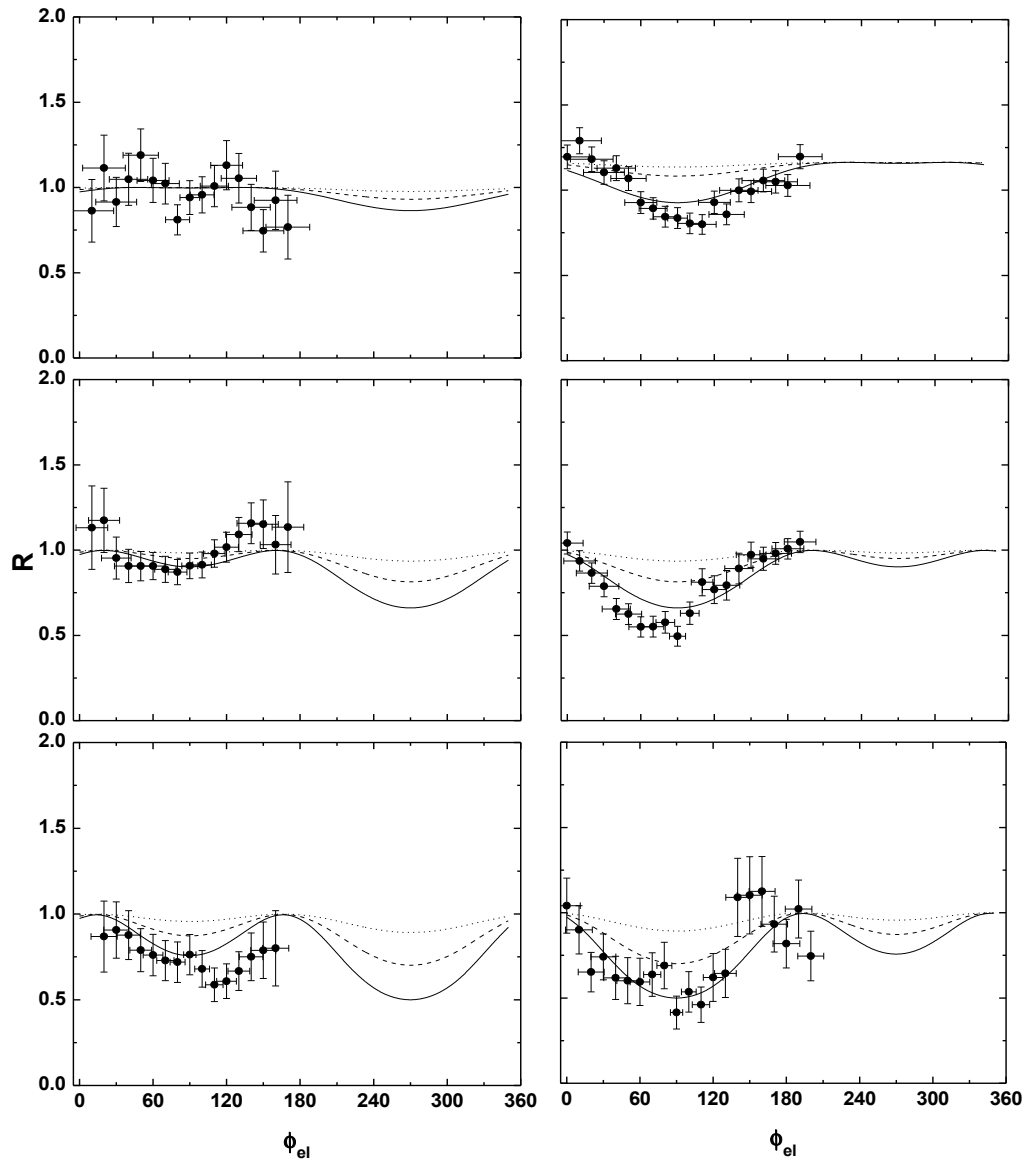


Figure 5: Fully differential cross section ratios between the large and small slit distance data of Fig. 4. The solid and dashed lines were obtained from $1 + \alpha \cos(q_x D)$ and equation (1) with $D = 2$ a.u. and 1.4 a.u., respectively, and the dotted curve from $1 + \alpha \sin(q_x D)/(q_x D)$ and $D = 1.4$ a.u.

and due to experimental resolution effects. In all cases the measured R are very well reproduced by this calculated I . The same interference term, multiplied by the incoherent FDCS, also reproduces the coherent FDCS for the scattering plane plotted in Fig. 3 (solid

curves). This supports the conclusion of ref. [20] suggesting that the phase angle in the interference term is primarily determined by q_x .

One important question to be answered is what implication of the dominance of q_x in the phase angle may be drawn regarding the type of interference that leads to the structures in R. As mentioned above, originally we believed that the interference was due to indistinguishable diffraction of the projectile wave from the two atomic centers in the molecule [13,16]. In this case the interference term was thought to be given by [25]

$$I = 1 + \cos(\mathbf{p}_{\text{rec}} \bullet \mathbf{d}) \quad (2a) \quad \text{or} \quad I = 1 + \sin(p_{\text{rec}}d)/(p_{\text{rec}}d) \quad (2b)$$

depending on whether the molecular orientation is fixed or random. Here, \mathbf{d} is the internuclear separation vector. Neither expression reproduces our measured R.

In ref. [20] we considered two possibilities to explain this observation. First, the phase angle in molecular two-center interference may not be primarily determined by \mathbf{p}_{rec} , but rather by q_x . But even then the dimension of the diffracting structure should still be given by the internuclear distance d , which is 1.4 a.u. for H_2 . Second, the dominant contribution to the interference may be due to some type other than two-center molecular interference. More specifically, we considered the possibility of first- and higher-order ionization amplitudes interfering with each other (to which we referred as single-center interference). Such interference contributions were also reported in coherent calculations [8,11]. The impact-parameters that contribute to the cross section at a specific scattering angle tend to be larger for first-order than for higher-order processes. This type of interference can therefore also be interpreted as due to different (indistinguishable) impact parameters leading to the same scattering angle. The requirement for observable interference is then that the transverse coherence length must be larger than the

separation in the impact-parameter distribution for the first- and higher order contributions. In order to test whether the FDCS are sensitive enough to distinguish between single- and two-center interference, in Fig. 5 expressions (2a) and (2b), with \mathbf{p}_{rec} replaced by q_x and $d = 1.4$ a.u. and the damping factor α inserted, are plotted as dashed and dotted curves, respectively. Equation (2a) assumes that the molecule is always aligned along q_x , which yields the most pronounced interference structure. Since the molecular orientation is not measured and we don't know whether the orientation is random, the measured R should be compared to the region between the dashed and dotted curves.

In most cases, the data seem to favor $D = 2$ a.u., i.e. single-center interference. However, the differences between both dimensions are not of sufficient significance to base a firm conclusion on them. Furthermore, it should be kept in mind that the data of ref. [20] suggested a rather weak, but not an absent dependence of the phase angle on p_{rec} . Therefore, a third possibility is that both two-center molecular (with the phase angle being determined by \mathbf{p}_{rec}) and single center interference are present in the data. The data strongly suggest that in this case the contributions from the latter would be larger.

Conclusions and outlook

In summary, we have performed a fully differential study of projectile coherence effects in ionization of H_2 . Differences in the measured cross sections depending on the transverse coherence length are confirmed by the present data. The ratio between the fully differential angular distributions of the ejected electrons for fixed energy and recoil-ion momentum for a coherent and an incoherent beam can be well described by an interference term in which the phase angle is primarily determined by the transverse

projectile momentum transfer. However, the FDCS are not sensitive enough to distinguish between two-center molecular and single-center interference. In order to shed more light on this important point we will perform further fully differential measurements varying kinematic parameters: first, we plan to repeat the experiment for a larger projectile energy loss and for a different initial projectile energy. Both parameters should have an effect on the impact parameter range contributing to ionization and thereby on the phase angle for single-center interference, while the internuclear separation of the molecule, which enters in the phase angle for two-center interference, is not affected. Second, we will measure FDCS for ionization of helium using proton beams of varying coherence length, for which molecular two-center interference obviously cannot contribute.

This work was supported by the National Science Foundation under grant no. PHY-1401586.

References

- [1] M. Schulz, R. Moshhammer, D. Fischer, H. Kollmus, D.H. Madison, S. Jones, and J. Ullrich, *Nature* **422**, 48 (2003)
- [2] R. Dörner, H. Khemliche, M.H. Prior, C.L. Cocke, J.A. Gary, R.E. Olson, V. Mergel, J. Ullrich, and H. Schmidt-Böcking, *Phys. Rev. Lett.* **77**, 4520 (1996)
- [3] N.V. Maydanyuk, A. Hasan, M. Foster, B. Tooke, E. Nanni, D.H. Madison, and M. Schulz, *Phys. Rev. Lett.* **94**, 243201 (2005)
- [4] M. Schulz, R. Moshhammer, A.N. Perumal, and J. Ullrich, *J. Phys. B* **35**, L161 (2002)
- [5] A.L. Harris, D.H. Madison, J.L. Peacher, M. Foster, K. Bartschat, and H.P. Saha *Phys. Rev. A* **75**, 032718 (2007)
- [6] M. McGovern, C.T. Whelan, and H.R.J. Walters, *Phys. Rev. A* **82**, 032702 (2010)
- [7] J. Colgan, M.S. Pindzola, F. Robicheaux, and M.F. Ciappina, *J. Phys. B* **44**, 175205 (2011)
- [8] A.B. Voitkiv, B. Najjari, and J. Ullrich, *J. Phys. B* **36**, 2591 (2003)
- [9] R.T. Pedlow, S.F.C. O'Rourke, and D.S.F. Crothers, *Phys. Rev. A* **72**, 062719 (2005)
- [10] M.F. Ciappina and W.R. Cravero, *J. Phys. B* **39**, 1091 (2006)
- [11] X.Y. Ma, X. Li, S.Y. Sun, and X.F. Jia, *Europhys. Lett.* **98**, 53001 (2012)
- [12] K.A. Kouzakov, S.A. Zaytsev, Yu.V. Popov, and M. Takahashi, *Phys. Rev. A* **86**, 032710 (2012)
- [13] K.N. Egodapitiya, S. Sharma, A. Hasan, A.C. Laforge, D.H. Madison, R. Moshhammer, and M. Schulz, *Phys. Rev. Lett.* **106**, 153202 (2011)
- [14] N. Stolterfoht, B. Sulik, V. Hoffmann, B. Skogvall, J. Y. Chesnel, J. Ragnama, F. Frémont, D. Hennecart, A. Cassimi, X. Husson, A. L. Landers, J. Tanis, M. E. Galassi, and R. D. Rivarola, *Phys. Rev. Lett.* **87**, 23201 (2001)

- [15] D. Misra, U. Kadhane, Y. P. Singh, L. C. Tribedi, P. D. Fainstein, and P. Richard
Phys. Rev. Lett. **92**, 153201 (2004)
- [16] J.S. Alexander, A.C. Laforge, A. Hasan, Z.S. Machavariani, M.F. Ciappina, R.D.
Rivarola, D.H. Madison, and M. Schulz, Phys. Rev. A **78**, 060701(R) (2008)
- [17] D. Misra, H.T. Schmidt, M. Gudmundsson, D. Fischer, N. Haag, H.A.B. Johansson,
A. Källberg, B. Najjari, P. Reinhed, R. Schuch, M. Schöffler, A. Simonsson, A.B.
Voitkiv, and H. Cederquist, Phys. Rev. Lett. **102**, 153201 (2009)
- [18] X. Wang, K. Schneider, A. LaForge, A. Kelkar, M. Grieser, R. Moshhammer, J.
Ullrich, M. Schulz, and D. Fischer, J. Phys. B **45**, 211001 (2012)
- [19] J.M. Feagin and L. Hargreaves, Phys. Rev. A **88**, 032705 (2013)
- [20] S. Sharma, T.P. Arthanayaka, A. Hasan, B.R. Lamichhane, J. Remolina, A. Smith,
and M. Schulz, Phys. Rev. A **89**, 052703 (2014)
- [21] A.D. Gaus, W. Htwe, J.A. Brand, T.J. Gay, and M. Schulz, Rev. Sci. Instrum. **65**,
3739 (1994)
- [22] H. Ehrhardt, K. Jung, G. Knoth, and P. Schlemmer, Z. Phys. D **1**, 3 (1986)
- [23] M. Schulz and D.H. Madison, International Journal of Modern Physics A **21**, 3649
(2006)
- [24] M. Dürr, B. Najjari, M. Schulz, A. Dorn, R. Moshhammer, A.B. Voitkiv, and J.
Ullrich, Phys. Rev. A **75**, 062708 (2007)
- [25] S.E. Corchs, R.D. Rivarola, J.H. McGuire, and Y.D. Wang, Phys. Scr. **50**, 469
(1994)

IV. Triple Differential Study of Ionization of H₂ by Proton Impact for Varying Electron Ejection Geometries

A. Hasan^{1,2}, S. Sharma¹, T.P. Arthanayaka¹, B.R. Lamichhane¹, J. Remolina¹, S. Akula¹, D.H. Madison¹, and M. Schulz¹

¹*Dept. of Physics and LAMOR, Missouri University of Science & Technology, Rolla, MO 65409*

²*Dept. of Physics, UAE University, P.O. Box 15551, Al Ain, Abu Dhabi, UAE*

Abstract

We have performed a kinematically complete experiment on ionization of H₂ by 75 keV proton impact. The triple differential cross sections (TDCS) extracted from the measurement were compared to a molecular 3-body distorted wave (M3DW) calculation for three different electron ejection geometries. Overall, the agreement between experiment and theory is better than in the case of a helium target for the same projectile. Nevertheless, significant quantitative discrepancies remain, which probably result from the capture channel, which may be strongly coupled to the ionization channel. Therefore, improved agreement could be expected from a non-perturbative coupled-channel approach.

Introduction

The description of the temporal and spatial evolution of a system as simple as three charged mutually interacting particles is a formidable theoretical challenge. Examples of such systems are ionization of atoms and molecules by electron or ion impact. The most sensitive experimental tests of theoretical models are offered by fully differential cross sections (FDCS), i.e. cross sections for which all independent kinematic parameters describing the system are fixed. For electron impact, FDCS for ionization of atomic targets have been obtained for several decades [e.g. 1-5 and references therein] by measuring the momentum vectors of two of the three particles and determining the third momentum vector from the kinematic conservation laws. The enormous challenge that theory is facing is reflected by the fact that only over the last 15 years satisfactory agreement with experiment was obtained even for the most simple target atoms [e.g. 6-8]. In the case of molecular targets the orientation of the internuclear axis represents an additional degree of freedom, which therefore has to be measured in addition to two momentum vectors in order to extract FDCS. Such experiments were only performed in recent years [9,10].

For ion impact, FDCS measurements are much more difficult because the much larger projectile mass results in extremely small (for heavy fast ions immeasurably small) scattering angles and energy losses relative to the initial energy. Only with the advent of cold target recoil-ion momentum spectroscopy (COLTRIMS) (for reviews see [11,12]) FDCS measurements for ion impact became feasible and since then numerous experiments were reported [e.g. 13-23]. Here, the agreement between experiment and theory is much less satisfactory [e.g. 24-26]. To the best of our knowledge no FDCS measurements have been performed yet for molecular targets. As far as the counterpart

to a FDCS experiment for atomic targets is concerned, i.e. the measurement of 2 momentum vectors, but not the molecular orientation, we are aware of only two reported experiments [27,28]. We refer to the cross sections extracted from these measurements as triple differential cross sections (TDCS) to distinguish them from truly fully differential data where the molecular orientation is fixed. In one of these studies the interest was focused on a molecular auto-ionization process, in which the electronic states are coupled to the nuclear motion [27]. The second experiment [28] was motivated by molecular interference effects which were reported earlier in double differential ejected electron [e.g. 29,30] and scattered projectile spectra [31].

About three years ago, we demonstrated that one important requirement to observe interference patterns in the projectile scattering angle dependence of the cross sections is that the projectile beam must be coherent, i.e. the dimension coherently illuminated by the projectile beam must be larger than the size of the diffracting object [32]. Such coherence effects were confirmed in several follow-up experiments and subsequently also observed in different collision systems and for other processes [28,33-36]. In these references the lack of transverse projectile coherence has been blamed for puzzling discrepancies between experiment and theory [e.g. 13] which were vividly debated for more than a decade. A thorough analysis of the role of the projectile coherence properties could therefore be quite important in order to advance our understanding of the few-body dynamics in atomic fragmentation processes. Furthermore, our recent studies on molecular targets revealed that in some cases the interference structures observed in the experimental spectra for a coherent projectile

beam, initially thought to be due to molecular two-center interference, are probably due to a different type (single-center) of interference [28,34].

In the study reported in this article our interest was not primarily focused on projectile coherence effects. Rather, the aim was to test the theoretical description of ionization of simple molecules by relatively slow proton impact. To this end we measured TDCS for a variety of different electron ejection geometries. Since theory assumes a coherent projectile beam the experiment was performed preparing a beam with a large coherence length.

Experiment

The experiment was performed at the Cockcroft-Walton accelerator of the Missouri University of Science & Technology. A proton beam was generated with a hot-cathode ion source and extracted through a 0.5 mm aperture. Other beam components were removed using a Wien filter. After focusing the beam by an electrostatic lens it was collimated by a second aperture with a diameter of 1.5 mm located 45 cm from the lens. The protons were accelerated to an energy of 75 keV. The beam was then further collimated by a pair of slits, oriented along the x- and y-directions, with a width of 150 μm located about 150 cm from the second aperture and 50 cm before the target. With this slit geometry a transverse coherence length of about 3.3 a.u. was realized, which is significantly larger than the inter-nuclear distance in H_2 of 1.4 a.u. The projectile beam was then intersected with a very cold ($T < 2$ K) H_2 beam from a supersonic gas jet. The beam component which did not charge exchange in collisions with the target or with the

rest gas (the vacuum throughout the beam line was better than 2.6×10^{-7} mbar) was selected by a switching magnet.

The scattered protons were decelerated to an energy of 5 keV, energy-analyzed using an electrostatic parallel plate analyzer [37], and detected by a two-dimensional position-sensitive micro-channel-plate (MCP) detector. The entrance and exit slits of the analyzer are very narrow ($\approx 75 \mu\text{m}$) in one direction (which we define to be the y -direction), but long ($\approx 2.5 \text{ cm}$) in the other direction, the x -direction. Therefore, for all detected protons the y -component of the momentum transfer \mathbf{q} was fixed at 0 (within the experimental resolution) and q_x was unambiguously determined by the x -position on the detector. To a very good approximation q_z is given by $q_z = \varepsilon/v_0$, where ε and v_0 are the energy loss and speed of the projectile, respectively. The energy resolution of the detected protons of 3 eV full width at half maximum (FWHM) corresponds to a resolution in q_z of 0.07 a.u. The resolution in q_x and q_y was 0.32 a.u. FWHM (corresponding to a scattering angle resolution of 0.1 mrad FWHM) and 0.2 a.u. FWHM, respectively.

The recoiling H_2^+ ions were extracted by a weak electric field (8V/cm) pointing in the x -direction over a distance of 10 cm before traversing a field-free drift region 20 cm in length. They were then detected also by a two-dimensional position-sensitive MCP detector which was set in coincidence with the projectile detector. From the position information the two momentum components in the plane perpendicular to the extraction field (the yz -plane) were obtained. The coincidence time yields the time-of-flight of the recoil ions from the collision region to the detector and thereby the x -component of the recoil-ion momentum.

To calibrate the recoil-ion momentum spectra, we also recorded coincidences between neutralized projectiles (detected by a second projectile detector) and recoil ions produced in a capture process. In this case the recoil momentum in the z-direction $p_{\text{rec}z}$ is given by $(I_i - I_f)/v_0 - v_0/2$ (where I_f and I_i are the ionization potentials of the target and the neutralized projectiles, respectively) and thus takes discrete values reflecting the final states of the captured electron. Since two capture lines could be resolved in the $p_{\text{rec}z}$ spectrum the calibration for this direction was straight-forward. The transformation factor from position to momentum for the y-direction is the same as for the z-direction because of the cylindrical symmetry of the COLTRIMS apparatus. The position corresponding to $p_{\text{rec}y} = 0$ can easily be determined by the required symmetry of the spectrum about $p_{\text{rec}y} = 0$ arising because the coincidences were recorded for all detected neutralized projectiles without any selection of \mathbf{q} . Finally, the recoil momentum spectrum in the x-direction was calibrated by analyzing the two-dimensional momentum spectrum in the xy-plane. Here, too, the integration over all \mathbf{q} leads to a required (circular) symmetry about $p_{\text{rec}x} = p_{\text{rec}y} = 0$. Therefore, the calibration parameters for the x-direction were obtained by generating a perfectly circular shape of the two-dimensional recoil momentum distribution. The momentum resolution in the x-, y-, and z-direction was 0.15, 0.5, and 0.15 a.u. FWHM, respectively. The relatively large resolution for the y-direction is mostly due to the target temperature, which is significantly larger in the direction of the gas expansion (y-direction) than in the plane perpendicular to the expansion.

Using momentum conservation the electron momentum is given by $\mathbf{p}_{\text{el}} = \mathbf{q} - \mathbf{p}_{\text{rec}}$. The TDCS will be presented differential in the solid angles of the projectiles and the

electrons and differential in the electron energy. Therefore, the electron momentum was converted from Cartesian to spherical coordinates in the data analysis software.

Results and Discussion

In Fig. 1 we present experimental (left panel) and theoretical (right panel) triple differential, three-dimensional angular distributions of the ejected electrons. The arrows labelled p_0 and q indicate the directions of the initial projectile momentum (which defines the positive z -axis) and of the momentum transfer (which lies in the xz plane and q_x defines the positive x -axis). These two vectors span the scattering plane and in the following we refer to the xy - and yz -planes as the azimuthal and perpendicular planes, respectively (note that these definitions are different than those often used in electron scattering). The electron energy is fixed at $E_{el} = 14.6$ eV and the magnitude of the

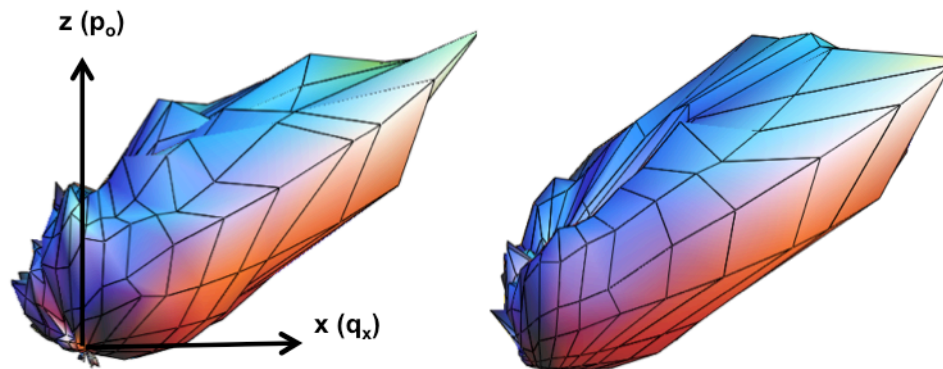


Figure 1: Experimental (left panel) and theoretical (right panel) three-dimensional plot of the triple differential cross sections for the electron energy fixed at 14.6 eV and the magnitude of the momentum transfer fixed at 0.9 a.u.

momentum transfer at 0.9 a.u. It should be noted that the recoil-ion momentum is typically of the same order of magnitude as the electron momentum. Since the mass of the recoil ion is 3 to 4 orders of magnitude larger than the electron mass the recoil-ion energy is negligible (a few meV or less). The projectile energy loss is then given by the

sum of the ejected electron energy and the ionization potential ($\epsilon = 30$ eV for $E_{e1} = 14.6$ eV). The calculation is based on the Molecular 3-Body Distorted Wave (M3DW) approach, which was described in detail previously [38].

The basic features in the experimental data are reproduced by theory. More specifically, a pronounced peak structure, approximately in the direction of \mathbf{q} (which is usually called the binary peak) is seen both in the measured and calculated plots. At the same time, neither in the experimental nor in the theoretical data significant contributions are observed in the direction of $-\mathbf{q}$, where often the so-called recoil peak is observed.

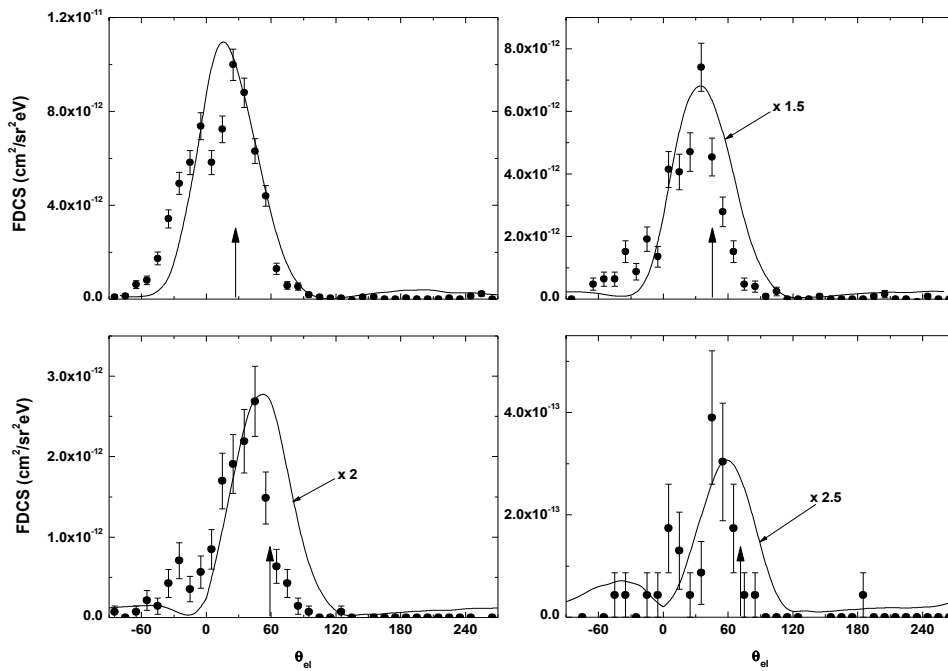


Figure 2: Triple differential cross sections for electrons with an energy of 14.6 eV ejected into the scattering plane as a function of the polar electron emission angle. The magnitude of the momentum transfer is fixed at 0.71 a.u. (upper left), 0.9 a.u. (upper right), 1.21 a.u. (lower left), and 1.86 a.u. (lower right). Solid curves: M3DW calculations (see text).

However, a closer inspection reveals some differences, as well. In the experimental plot a “shoulder” can be seen in the region of negative p_{elx} and positive p_{elz} , which is not present in the calculation. Furthermore, the binary peak in the experimental plot as a function of the polar angle (measured clockwise relative to the z-axis in the coordinate system of Fig. 1) appears to be somewhat narrower than in the theoretical plot. In order to analyze these discrepancies in more detail, we will discuss cuts of selected electron ejection planes through the three-dimensional TDCS.

In Fig. 2 we show TDCS for electrons with an energy of 14.6 eV ejected into the scattering plane as a function of the polar electron ejection angle θ_{el} (where 0° to 180° is on the binary peak side of the scattering plane and 180° to 360° is on the recoil peak side). The magnitude of the momentum transfer was fixed at 0.71 a.u. (upper left), 0.9 a.u. (upper right), 1.21 a.u. (lower left), and 1.86 a.u. (lower right). The arrow indicates the direction of \mathbf{q} in each case and the solid curves show our M3DW calculations. The shape of the angular dependence of the TDCS has some features in common with corresponding data which we obtained earlier for 75 keV p + He collisions [14,39]: a) With increasing q the centroid of the binary peak is increasingly shifted in the forward direction relative to \mathbf{q} . b) No recoil peak is observed for any q , while for many other collision systems a clear recoil peak is visible at least for small q [13,16-21]. c) With increasing q the experimental binary peak becomes increasingly narrow relative to the theoretical widths. d) The shoulder in the binary peak, or even separate peak structure, in the region of negative p_{elx} and positive p_{elz} , mentioned in the context of Fig. 1 already, decreases in intensity (relative to the binary peak) with increasing q

The forward shift relative to \mathbf{q} is due to the post-collision interaction (PCI) between the scattered projectile and the outgoing electron which was already raised to the

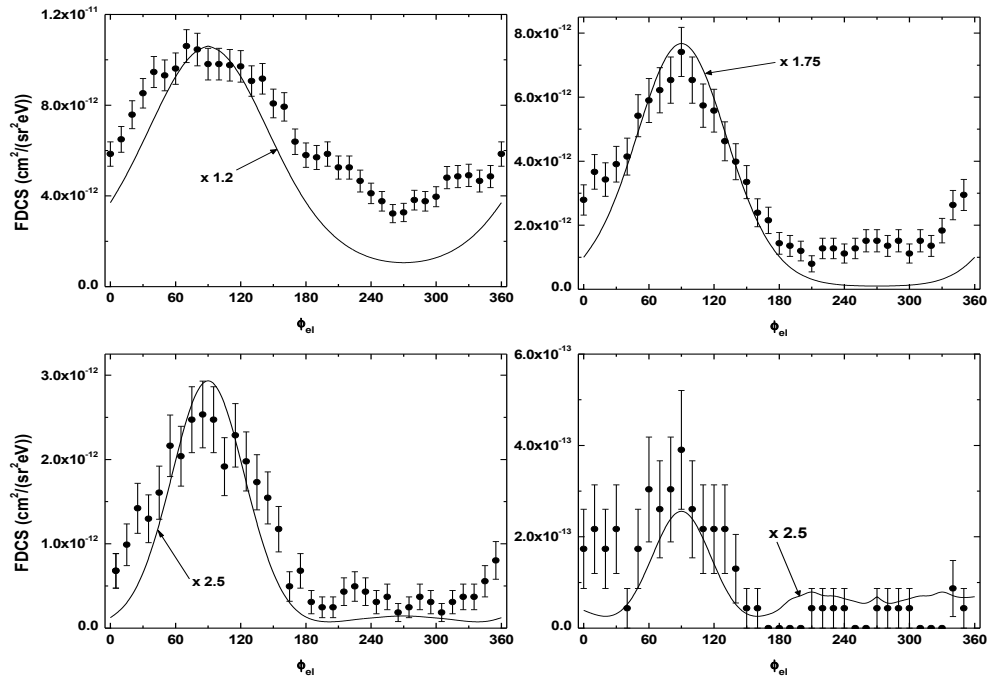


Figure 3: Triple differential cross sections for electrons with an energy of 14.6 eV ejected along the surface of a cone with an opening angle of 35° (45° for $q = 1.86$ a.u.) as a function of the azimuthal electron emission angle. q was fixed at the same values as in Fig. 2. Solid curves as in Fig. 2.

continuum by a preceding primary interaction with the projectile. A recent systematic study of PCI as a function of q revealed that it becomes increasingly important with increasing q [21], in accordance with the present data and those of refs. 14 and 39. Regarding the absence of the recoil peak, it was already demonstrated about a decade ago that it can be strongly suppressed by a combination of PCI and the projectile – target nucleus interaction [40]. A peak structure in the region of negative p_{elx} and positive p_{elz} was also observed in calculations for target ionization by highly-charged ion impact [41].

It was interpreted, using a classical picture, in terms of a higher-order process in which the projectile passes the target nucleus at the opposite side from the location of the active electron. The target nucleus and the electron are then deflected in opposite directions by their interaction with the projectile. Since the nucleus is closer to the projectile than the electron, it suffers a larger deflection and thus primarily determines the direction of \mathbf{q} . The electron will therefore be ejected with a momentum in the x -direction opposite to q_x (i.e. $p_{\text{el}x} < 0$). At present we cannot offer an explanation for the smaller width of the binary peak compared to theory. However, overall the data of Fig. 2 seem to be consistent with previous data and also with our current understanding of the reaction dynamics in ionizing collisions.

The qualitative agreement between theory and experiment is satisfactory in so far as the position of the binary peak is reasonably reproduced and that a negligibly small recoil peak (compared to the binary peak) is confirmed by theory. However, there are also some significant discrepancies: a) Except for the smallest q the absolute overall magnitude is smaller in the calculation by a factor ranging from 1.5 for $q = 0.9$ a.u. and 2.5 for the largest q . b) As mentioned already, the width of the binary peak is overestimated by theory. c) The shoulder on the left wing of the binary peak in the calculation becomes more pronounced with increasing q , while in the measured data it becomes more important with decreasing q . Nevertheless, and somewhat surprising considering that H_2 is more complex than He, the overall agreement between theory and experiment is notably better than for 75 keV $p + \text{He}$ collisions [14,39].

The three-dimensional plots of Fig. 1 show that the TDCS for electron ejection into the azimuthal plane is very small. Therefore, in order to study the dependence of the

TDCS on the azimuthal electron ejection angle ϕ_{el} , we present in Fig. 3 data for the polar electron angle fixed at $\theta_{el} = 35^\circ$, rather than $\theta_{el} = 90^\circ$, which would select the azimuthal plane, and for q fixed at the same values as in Fig. 2. For the largest q the TDCS maximize around $\theta_{el} = 45^\circ$ and here the polar angle is fixed at this value. This corresponds to a geometry in which all electrons are emitted along the surface of a cone with an opening angle of 35° or 45° , respectively, about the projectile beam axis. The azimuthal angular axis in the plots of Fig. 3 is unconventional in so far as ϕ_{el} is the angle between the projection of \mathbf{p}_{el} onto the xy -plane and the positive y -axis, rather than the positive x -axis. With this convention $\phi_{el} = 90^\circ$ coincides with the direction of the transverse component of \mathbf{q} (i.e. q_x).

The ϕ_{el} – dependence of the TDCS for emission along this conical surface is once again dominated by the binary peak at 90° . Nevertheless, the TDCS near 270° (which coincides with the direction of $-q_x$), i.e. in the region where the recoil peak is often observed, is significantly larger than in the scattering plane. However, there is still no peak structure and, in fact, for $q = 0.7$ a.u. a minimum is found at 270° . The relatively large cross section in this region is mostly due to the significantly larger width of the binary peak in the ϕ_{el} – dependence compared to the θ_{el} – dependence. This difference in width, in turn, is a clear signature of significant higher-order contributions because in a first-order treatment the TDCS must be cylindrically symmetric about \mathbf{q} .

The agreement between theory and experiment for the ϕ_{el} – dependence of the TDCS is somewhat better than for the scattering plane. As far as the overall magnitude is concerned the discrepancies for both geometries are about the same. However, the width of the binary peak in the experimental data is much better reproduced by theory for the ϕ_{el}

– dependence, although it is still underestimated in the case of $q = 0.7$ a.u. On the other hand, in the region $\phi_{el} = 180^\circ$ to 360° , the theoretical TDCS (after adjusting the magnitude to match the binary peak) is too small for the two smaller values of q . Recall that the condition $\theta_{el} = 35^\circ$ (or 45°) selects electron momenta with positive p_{elz} . Therefore, the contributions in this angular region (for which $p_{elx} < 0$) are part of the shoulder to the binary peak which we discussed already in the context of the three-

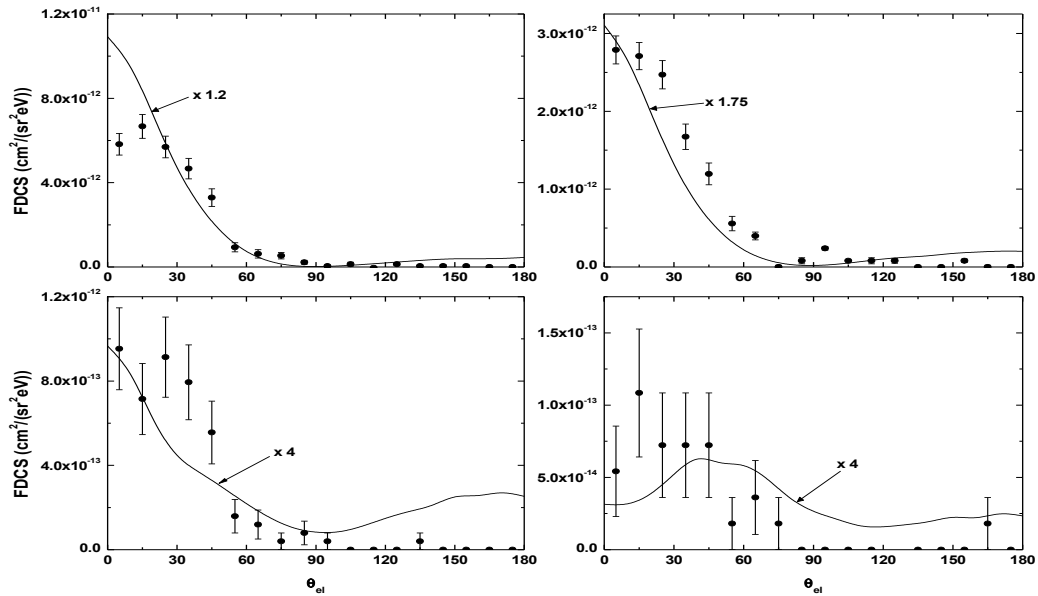


Figure 4: Same as Fig. 2 for electron ejection into the perpendicular plane.

dimensional plots and which we explained in terms of a higher-order process involving the projectile – target nucleus interaction. The discrepancies in this region are thus indicative for an incomplete description of such higher-order contributions. Fully differential data for other collision systems have previously led us to similar conclusions [e.g. 14,17,39].

Finally, in Fig. 4 we present the TDCS for electrons ejected into the perpendicular plane, again for the same values of q as in Fig. 2. Basically, the cross sections drop monotonically and steeply with increasing θ_{el} . Similar to the scattering plane, here too the shape of the angular dependence is analogous to 75 keV p + He collisions [39]. For this geometry we obtain the worst agreement between experiment and theory. The discrepancies in the overall magnitude are larger than for the other two cases, especially for the two largest values of q . Furthermore, theory predicts maxima at $\theta_{el} = 180^\circ$, especially for large q , which are not present in the data. Finally, the decrease in the TDCS with increasing θ_{el} is even steeper than in the measured data, especially at small q . At $q = 1.86$ a.u., theory predicts another peak structure around $\theta_{el} = 45^\circ$. The error bars in the experimental TDCS for this q are too large to determine whether there is a maximum at $\theta_{el} > 0$.

Conclusions

We have measured and calculated triple differential cross sections for ionization of H_2 by 75 keV p impact for three different electron ejection geometries. Pronounced signatures of higher-order contributions, especially those involving the projectile – target nucleus interaction, are seen in the data, which is not surprising for the relatively large perturbation parameter η (projectile charge to speed ratio) of 0.6. The comparison between experiment and theory shows reasonable qualitative agreement, but there are also substantial quantitative discrepancies. Considering that the calculation is based on a perturbative approach, these discrepancies may not seem all that surprising. However, it should be noted that η is not the only important factor for the range of validity of a theoretical model. In fact, for fast, highly charged ion impact at similar (or even larger) η

better agreement with perturbative methods accounting for higher-order effects has been achieved [e.g. 18,42]. One important difference for the collision system studied here is that due to the low projectile charge state the same η corresponds to a much smaller projectile speed than for highly charged ions. This, in turn, means that the capture channel, which may be strongly coupled to the ionization channel and for which the cross section strongly depends on the projectile speed, becomes much more important. The present results thus suggest that in the kinematic regime studied here numerically improved agreement could be obtained by a non-perturbative coupled-channel approach.

Acknowledgements

This work was supported by the National Science Foundation under grant nos. PHY- 1401586 and PHY-1068237 and by TeraGrid resources provided by the Texas Advanced Computing Center (Grant No. TG-MCA07S029).

References

- [1] H. Ehrhardt, M. Schulz, T. Tekaats, and K. Willmann, *Phys. Rev. Lett.* 22, 89 (1969)
- [2] A.J. Murray, M.B.J. Woolf, and F.H. Read, *J. Phys. B* 25, 3021 (1992)
- [3] J. Röder, H. Ehrhardt, I. Bray, D.V. Fursa, I.E. McCarthy, *J. Phys. B* 29, 2103 (1996)
- [4] M. Dürr, C. Dimopoulou, A. Dorn, B. Najjari, I. Bray, D.V. Fursa, Zhangjin Chen, D.H. Madison, K. Bartschat, and J. Ullrich, *J. Phys. B* 39, 4097 (2006)
- [5] A. Lahmam-Bennani, E.M. Staicu Casagrande, and A. Naja, *J. Phys. B* 42, 235205 (2009)
- [6] T.N. Rescigno, M. Baertschy, W.A. Isaacs, and C.W. McCurdy, *Science* 286, 2474 (1999)
- [7] I. Bray, *Phys. Rev. Lett.* 89, 273201 (2002)
- [8] S. Amami, M. Ulu, Z.N. Ozer, M. Yavuz, S. Kazgoz, M. Dogan, O. Zatsarinny, K. Bartschat, and D.H. Madison, *Phys. Rev. A* 90, 012704 (2014).
- [9] X. Ren, T. Pflüger, S. Xu, J. Colgan, M. S. Pindzola, A. Senftleben, J. Ullrich, and A. Dorn, *Phys. Rev. Lett.* 109, 123202 (2012)
- [10] S. Bellm, J. Lower, E. Weigold, and D. W. Mueller, *Phys. Rev. Lett.* 104, 023202 (2010)
- [11] R. Dörner, V. Mergel, O. Jagutzki, L. Spielberger, J. Ullrich, R. Moshhammer, and H. Schmidt-Böcking, *Phys. Rep.* 330, 95 (2000)
- [12] J. Ullrich, R. Moshhammer, A. Dorn, R. Dörner, L. Schmidt, and H. Schmidt-Böcking, *Rep. Prog. Phys.* 66, 1463 (2003)
- [13] M. Schulz, R. Moshhammer, D. Fischer, H. Kollmus, D.H. Madison, S. Jones, and J. Ullrich, *Nature* 422, 48 (2003)

- [14] N.V. Maydanyuk, A. Hasan, M. Foster, B. Tooke, E. Nanni, D.H. Madison, and M. Schulz, *Phys. Rev. Lett.* 94, 243201 (2005)
- [15] L. An, K. Khayyat, and M. Schulz, *Phys. Rev. A* 63, 030703 (2001)
- [16] M. Schulz, R. Moshhammer, D.H. Madison, R.E. Olson, P. Marchalant, C.T. Whelan, S. Jones, M. Foster, H. Kollmus, A. Cassimi, and J. Ullrich, *J. Phys.* B34, L305 (2001)
- [17] M. Schulz, R. Moshhammer, A.N. Perumal, and J. Ullrich, *J. Phys. B* 35, L161 (2002)
- [18] D. Fischer, R. Moshhammer, M. Schulz, A. Voitkiv, and J. Ullrich, *J. Phys. B* 36, 3555 (2003)
- [19] A.B. Voitkiv, B. Najjari, R. Moshhammer, M. Schulz, and J. Ullrich, *J. Phys. B* 37, L365 (2004)
- [20] M. Schulz, R. Moshhammer, A. Voitkiv, B. Najjari, and J. Ullrich, *Nucl. Instrum. Meth. B* 235, 296 (2005)
- [21] M. Schulz, B. Najjari, A.B. Voitkiv, K. Schneider, X. Wang, A.C. Laforge, R. Hubele, J. Goullon, N. Ferreira, A. Kelkar, M. Grieser, R. Moshhammer, J. Ullrich, and D. Fischer, *Phys. Rev. A* 88, 022704 (2013)
- [22] R. Hubele, A.C. Laforge, M. Schulz, J. Goullon, X. Wang, B. Najjari, N. Ferreira, M. Grieser, V.L.B. de Jesus, R. Moshhammer, K. Schneider, A.B. Voitkiv, and D. Fischer, *Phys. Rev. Lett.* 110, 133201 (2013)
- [23] M. Schulz and D.H. Madison, *International Journal of Modern Physics A* 21, 3649 (2006)
- [24] M. McGovern, D. Assafrão, J. R. Mohallem, C.T. Whelan, and H.R.J. Walters *Phys. Rev. A* 81, 042704 (2010)

- [25] K.A. Kouzakov, S.A. Zaytsev, Yu.V. Popov, and M. Takahashi, *Phys. Rev. A* 86, 032710 (2012)
- [26] M. F. Ciappina, W. R. Cravero, and M. Schulz, *J. Phys. B* 40, 2577 (2007)
- [27] C. Dimopoulou, R. Moshhammer, D. Fischer, C. Höhr, A. Dorn, P.D. Fainstein, J.R. Crespo López Urrutia, C.D. Schröter, H. Kollmus, R. Mann, S. Hagmann, and J. Ullrich, *Phys. Rev. Lett.* 93, 123203 (2004)
- [28] S. Sharma, T.P. Arthanayaka, A. Hasan, B.R. Lamichhane, J. Remolina, A. Smith, and M. Schulz, submitted to *Phys. Rev. A* (2014)
- [29] N. Stolterfoht, B. Sulik, V. Hoffmann, B. Skogvall, J.Y. Chesnel, J. Ragnama, F. Frèmont, D. Hennecart, A. Cassimi, X. Husson, A.L. Landers, J. Tanis, M.E. Galassi, and R.D. Rivarola, *Phys. Rev. Lett.* 87, 23201 (2001)
- [30] D. Misra, A. Kelkar, U. Kadhane, A. Kumar, L.C. Tribedi, and P.D. Fainstein, *Phys. Rev. A* 74, 060701 (2006)
- [31] J.S. Alexander, A.C. Laforge, A. Hasan, Z.S. Machavariani, M.F. Ciappina, R.D. Rivarola, D.H. Madison, and M. Schulz, *Phys. Rev. A* 78, 060701 (2008)
- [32] K.N. Egodapitiya, S. Sharma, A. Hasan, A.C. Laforge, D.H. Madison, R. Moshhammer, and M. Schulz, *Phys. Rev. Lett.* 106, 153202 (2011)
- [33] X. Wang, K. Schneider, A. LaForge, A. Kelkar, M. Grieser, R. Moshhammer, J. Ullrich, M. Schulz, and D. Fischer, *J. Phys. B* 45, 211001 (2012)
- [34] S. Sharma, A. Hasan, K.N. Egodapitiya, T. P. Arthanayaka, and M. Schulz, *Phys. Rev. A* 86, 022706 (2012)
- [35] K. Schneider, M. Schulz, X. Wang, A. Kelkar, M. Grieser, C. Krantz, J. Ullrich, R. Moshhammer, and D. Fischer, *Phys. Rev. Lett.* 110, 113201 (2013)

- [36] S. Sharma, T.P. Arthanayaka, A. Hasan, B.R. Lamichhane, J. Remolina, A. Smith, and M. Schulz, *Phys. Rev. A* 89, 052703 (2014)
- [37] A.D. Gaus, W. Htwe, J.A. Brand, T.J. Gay, and M. Schulz, *Rev. Sci. Instrum.* 65, 3739 (1994)
- [38] U. Chowdhury, M. Schulz, and D. H. Madison, *Phys. Rev. A* 83, 032712 (2011)
- [39] M. Schulz, A. Hasan, N.V. Maydanyuk, M. Foster, B. Tooke, and D.H. Madison, *Phys. Rev. A* 73, 062704 (2006)
- [40] A. Hasan, N.V. Maydanyuk, B.J. Fendler, A. Voitkiv, B. Najjari, and M. Schulz, *J. Phys. B* 37, 1923 (2004)
- [41] J. Fiol and R.E. Olson, *J. Phys. B* 35, 1759 (2002)
- [42] D.H. Madison, D. Fischer, M. Foster, M. Schulz, R. Moshhammer, S. Jones, and J. Ullrich *Phys. Rev. Lett.* 91, 253201 (2003)

SECTION

2. CONCLUSIONS

This dissertation is comprised of four papers. The essence of the experimental method used in the first three papers is that the width of the projectile wave-packet could be controlled by the geometry of a collimating slit placed before the target region. Consequently, a projectile beam could be prepared where width of the projectile wave-packet is either larger (coherent) or smaller (incoherent) than the target dimensions. Paper I describes an experimental study of projectile coherence effects for single electron capture from H_2 and He by proton impact. Differential cross sections (DCS) for single capture from a diatomic molecular target H_2 by 25 and 75 keV protons and from a monoatomic target He by 25 keV protons were measured as a function of the projectile scattering angle. Significant differences between the coherent and the incoherent DCS were observed for all of the above-mentioned cases. For 75 keV $p + H_2$, the coherent DCS (DCS_{coh}) oscillate about the incoherent DCS (DCS_{inc}). This pattern was interpreted as due to molecular two-center interference.

For 25 keV $p + H_2$, the DCS_{coh} were also observed to be significantly different than DCS_{inc} , which further confirms the importance of the projectile coherence properties. However, in this case the IT was qualitatively different as compared to 75 keV $p + H_2$. For 25 keV $p + He$, clear differences between DCS_{coh} and DCS_{inc} were observed as well. Surprisingly, the IT in the case of He (atomic target) was observed to be very

similar to 25 keV $p + H_2$ (molecular target). This suggests that the interference effects for the 25 keV cases could not be described by molecular two-center interference. Although, the contributions from two-center interference couldn't be entirely ruled out for 25 keV $p + H_2$, the similarity between IT for an atomic and the H_2 target indicates that this is at least not the dominant contribution. The same conclusion can also be drawn for dissociative capture in 25 keV $p + H_2$ collisions, for which IT also closely resembles the one for capture from He.

In paper I we proposed that the dominant interference observed for a projectile energy of 25 keV is due to a coherent superposition of first- and higher-order transition amplitudes (especially those involving the projectile – target nucleus interaction), to which we referred as single-center interference. An analogous interpretation for the case of ionization of helium by fast ion impact has been supported by recent FDCS measurements for proton impact [38]. This idea was further pursued in paper II, which describes a kinematically complete experiment on single ionization of H_2 by 75 keV proton impact. While significant differences between the coherent and incoherent DDCS as a function of projectile angles (θ) were confirmed, only small differences were found in the recoil-ion and electron momentum dependence of the measured cross sections. This shows that the phase angle in the IT is primarily determined by the momentum transfer rather than by the recoil-ion momentum. Since the phase angle for molecular two-center interference is believed to be determined by the recoil-ion momentum, this is indicative that in ionization of H_2 , as in capture by 25 keV proton impact, single center interference dominates over two-center interference. However, an alternative explanation, which cannot be ruled out yet (at least not on the basis of the data presented

in this thesis), is that even in molecular two-center interference the phase angle is not primarily determined by the recoil-ion momentum.

Another important conclusion presented in paper II is related to a theoretical analysis which was recently presented by Feagin and Hargreaves. Although they acknowledged that projectile coherence properties can influence measured cross sections, they argued that this should not be viewed as wave-packet (de)coherence. Rather, they asserted that the DDCS measured for an incoherent beam can be reproduced by averaging the cross sections for an entirely coherent beam over the complete range of angles subtended by the collimating slit at the target. However, in this analysis they had to assume that the angular spread in the incoming projectile beam for the incoherent beam had to be about 2 mrad in order to reproduce the experimental data. In order to test their analysis they suggested to not only measure the projectile scattering angle directly, but to also determine it from the sum of the electron and recoil-ion momenta. If the DDCS for the coherent and incoherent projectiles were then extracted with the additional conditions that the scattering angle measured directly and determined from the target fragments were the same the differences in these cross sections, Feagin and Hargreaves argued, should go away. This test was performed and it was found that a) there was no significant difference in the resolution between the coherent and the incoherent beam, b) the resolution was about an order of magnitude better than what was assumed by Feagin and Hargreaves for the incoherent beam and that c) the condition consequently had no significant effect on the comparison between measured DDCS for a coherent and an incoherent beam. The results of this test thus clearly demonstrate that the explanation of Feagin and Hargreaves for the differences between the DDCS for a coherent and an incoherent beam is not

correct and that these differences are clearly not merely due to experimental resolution effects.

In paper three, FDCS measurements have been reported for single ionization of H_2 by 75 keV proton impact. Here, fully differential, three-dimensional ejected electron momentum spectra (for fixed q) were deduced for a coherent and an incoherent projectile beam. The differences between coherent and incoherent FDCS were found to be very weak. In the previous paper it was inferred that the ratios between the coherent and incoherent cross section seem to be sensitive to momentum transfer rather than the recoil-ion momentum. Therefore, the FDCS were measured for fixed p_{rec} , so that variations in cross sections alongside q could be analyzed. It was observed that in the θ_{el} dependence, the coherent and incoherent cross sections were narrowly distributed, which makes it difficult to observe differences between them. Therefore, the ϕ_{el} dependence of the cross sections was analyzed for fixed polar angles of the ejected electron. Here, clear variations between the coherent and incoherent FDCS were observed and the differences enhanced significantly with increasing θ_{el} . As of now there are no theoretical studies that relate the IT with momentum transfer, however, a simple model is presented, which predicts that the momentum transfer determines the phase angle in the IT for single center interference. The experimental data were compared to the $IT = 1 + \alpha \cos(q_t D)$. A best fit of IT to the experimental data is obtained using $D = 2$ a.u., which corresponds to the average difference between impact parameters for the first and higher order contributions. Although, the FDCS do not provide conclusive evidence, the IT for single-center interference seems to reproduce the experimental data better than for two-center

interference. Therefore, various experimental studies have been considered for further analysis of these effects and are discussed below.

In Paper IV, the FDCS for varying electron ejection geometries were reported for ionization of H_2 by 75 keV proton impact. Rather than the projectile coherence properties, this study focuses primarily on the understanding of few-body aspects through FDCS measurements and their comparison with theoretical results. In this study, only coherent cross sections were discussed because the theoretical model which the data were compared to assume a coherent projectile beam. Signatures of higher order contributions were observed in the three dimensional angular distribution of ejected electron momenta. The ejected electron momentum distribution was observed to be asymmetric about \mathbf{q} in the scattering plane. In contrast, for a first-order process this distribution should be symmetric about \mathbf{q} . In the scattering plane it was observed that, qualitatively, the molecular 3-body distorted wave (M3DW) calculations reasonably reproduce the experimental data. However, quantitatively, the cross sections differ significantly. It was also observed that with increasing momentum transfer the binary peak shifts increasingly in the forward direction relative to \mathbf{q} . These results are interpreted in terms of the post collision interactions (PCI), between the scattered projectile and the ejected electron, becoming increasingly important with increasing q and similar behavior was also observed for ionization of He and Li [39]. In the perpendicular plane and azimuthal plane too, the experimental data are qualitatively well reproduced but the quantitative discrepancies are significant. Essentially, perturbative models with similar η , that incorporate higher order effects, have been able to reproduce experimental data for collisions with very fast projectiles reasonably well. However, one major reason for these

discrepancies in current experimental study may be the capture channel that could be strongly coupled to ionization channel due to lower projectile speed. Thus, these discrepancies are expected to be addressed better by a non-perturbative coupled-channel approach. For fast ion impact, in contrast, the capture channel is entirely negligible because of the very steep decrease of the capture cross sections with increasing projectile energy.

In order to probe interference effects further, different experimental studies, that are capable of distinguishing between one-center and two-center interference effects, are intended to be performed. Therefore, two possibilities have been considered. First, the ionization of H_2 will be studied by 75 keV proton impact, for larger projectile energy losses. On average, larger energy losses result from collisions with smaller impact parameters. Consequently, relative to single-center interference the effective size of the target entering in the phase angle is reduced. In contrast, for two-center interference the effective size of the target is determined by the inter-nuclear separation of the molecule, which remains the same regardless of the energy loss of the projectile. Second, a kinematically complete study on ionization of He (an atomic target) by 75 keV protons with varied coherence length is intended to be performed. The advantage of this study is that molecular two-center interference can be entirely ruled out. Therefore, if differences between coherent and incoherent cross sections still persist these can clearly be associated with single-center interference. These experimental studies are ongoing and are expected to further enhance our knowledge about projectile coherence effects in near future.

BIBLIOGRAPHY

- [1] M. Schulz, R. Moshhammer, D. Fischer, H. Kollmus, D. H. Madison, S. Jones, and J. Ullrich, *Nature* **422** 48 (2003)
- [2] T.N. Rescigno, M. Baertschy, W.A. Isaacs, and C.W. McCurdy, *Science* **286**, 2474 (1999)
- [3] H. Ehrhardt, M. Schulz, T. Tekaats, and K. Willmann, *Phys. Rev. Lett.* **22**, 89 (1969)
- [4] H. Ehrhardt, K. Jung, G. Knoth, and P. Schlemmer, *Z. Phys. D*, (1986)
- [5] I. Bray, *J. Phys.* **B33**, 581 (2000)
- [6] J. Colgan, M. S. Pindzola, *Phys. Rev. A* **74**, 012713 (2006)
- [7] M. Schulz, M. F. Ciappina, T. Kirchner, D. Fischer, R. Moshhammer, and J. Ullrich, *Phys. Rev. A* **79**, 042708 (2009)
- [8] M. Schulz, *Phys. Scr.* **80**, 068101 (2009)
- [9] R. Dörner, V. Mergel, R. Ali, U. Buck, C.L. Cocke, K. Froschauer, O. Jagutzki, S. Lencinas, W.E. Meyerhof, S. Nüttgens, R. E. Olson, H. Schmidt-Böcking, L. Spielberger, K. Tökesi, J. Ullrich, M. Unverzagt, and W. Wu, *Phys. Rev. Lett.* **72**, 3166 (1994)
- [10] J. Ullrich, R. Moshhammer, R Dörner, O. Jagutzki, V. Mergel, H. Schmidt-Böcking and L. Spielberger, *J. Phys. B* **30**, 2917 (1997)
- [11] R. Moshhammer, M. Unverzagt, W. Schmitt, J. Ullrich, and H. Schmidt-Böcking, *Nucl. Instrum. Methods Phys. Res. B* **108**, 425 (1996)
- [12] M. F. Ciappina et al., *Phys. Rev. A* **74**, 042702 (2006)
- [13] A. B. Voitkiv and B. Najjari, *Phys. Rev. A* **79**, 022709 (2009)
- [14] D.H. Madison et al., *Phys. Rev. Lett.* **91**, 253201 (2003)
- [15] R. E. Olson and J. Fiol, *Phys. Rev. Lett.* **95**, 263203 (2005)
- [16] J. Fiol, S. Otranto, and R. E. Olson, *J. Phys. B* **39**, L285 (2006)
- [17] M. Dürr, B. Najjari, M. Schulz, A. Dorn, R. Moshhammer, A. B. Voitkiv, and J. Ullrich, *Phys. Rev. A*, **75**, 062708 (2007)
- [18] M. Schulz, M. Dürr, B. Najjari, R. Moshhammer, and J. Ullrich, *Phys. Rev. A* **76**, 032712 (2007)

- [19] D Madison, M Schulz, S Jones¹, M Foster, R Moshhammer and J Ullrich, *J. Phys. B* **35** (2002)
- [20] D. H. Madison, D. Fischer, M. Foster, M. Schulz, R. Moshhammer, S. Jones, and J. Ullrich, *Phys. Rev. Lett.* **91**, 253201 (2003)
- [21] I. B. Abdurakhmanov, I. Bray, D. V. Fursa, A. S. Kadyrov, and A. T. Stelbovics, *Phys. Rev. A* **86**, 034701 (2012)
- [22] M. S. Pindzola and F. Robicheaux, *Phys. Rev. A* **82**, 042719 (2010)
- [23] K. N. Egodapitiya, S. Sharma, A. Hasan, A. C. Laforge, D. H. Madison, R. Moshhammer, and M. Schulz, *Phys. Rev. Lett.* **106**, 153202 (2011)
- [24] J. S. Alexander, A. C. Laforge, A. Hasan, Z. S. Machavariani, M. F. Ciappina, R. D. Rivarola, D. H. Madison, and M. Schulz, *Phys. Rev. A* **78**, 060701(R) (2009)
- [25] T. F. Tuan and E. Gerjuoy, *Phys. Rev.* **117**, 756 (1960)
- [26] H. D. Cohen and U. Fano, *Phys. Rev.* **150** (1966)
- [27] S. Cheng, C. L. Cocke, V. Frohne, E. Y. Kamber, J. H. McGuire, and Y. Wang, *Phys. Rev. A* **47**, 3923-3929 (1993)
- [28] N. Stolterfoht, B. Sulik, V. Hoffmann, B. Skogvall, J. Y. Chesnel, J. Rangama, F. Frémont, D. Hennecart, A. Cassimi, X. Husson, A. L. Landers, J. A. Tanis, M. E. Galassi, and R. D. Rivarola, *Phys Rev. Lett.* **87**, 023201 (2001)
- [29] D. Misra, A. Kelkar, U. Kadhane, Ajay Kumar, Y. P. Singh, and Lokesh C. Tribedi, *Phys. Rev. A* **75**, 052712 (2007)
- [30] K. Støchkel, O. Eidem, H. Cederquist, H. Zettergren, P. Reinhed, R. Schuch, C. L. Cocke, S. B. Levin, *Phys. Rev. A* **72**, 050703(R) (2005)
- [31] A. L. Landers, E. Wells,³ T. Osipov, K. D. Carnes, A. S. Alnaser, J. A. Tanis, J. H. McGuire, I. Ben-Itzhak, and C. L. Cocke, *Phys. Rev. A* **70**, 042702 (2004)
- [32] S. Mondal and R. Shankar, *Phys. Rev. A* **69**, 060701(R) (2004)
- [33] L. Ph. H. Schmidt, S. Schössler, F. Afaneh, M. Schöffler, K.E. Stiebing, H. Schmidt-Böcking, and R. Dörner, *Phys. Rev. A* **101**, 173202 (2008)
- [34] S. F. Zhang, D. Fischer,² M. Schulz, A. B. Voitkiv, A. Senftleben, A. Dorn, J. Ullrich, X. Ma, and R. Moshhammer, *Phys. Rev. Lett.* **112**, 023201 (2014)
- [35] A. Messiah, *Quantum Mechanics Vol. 2*

- [36] C. Keller, Jorg Schmiedmayer, and A. Zeilinger, *Optics Communications* **179**, 129-135 (2000).
- [37] A.C. Laforge, K.N. Egodapitiya, J.S. Alexander, A. Hasan, M.F. Ciappina, M.A. Khakoo, and M. Schulz, *Phys. Rev. Lett.* **103**, 053201 (2009)
- [38] X. Wang, K. Schneider, A. LaForge, A. Kelkar, M. Grieser, R. Moshhammer, J. Ullrich, M. Schulz and D Fischer, *J. Phys. B* **45**, 211001 (2012)
- [39] M. Schulz, B. Najjari, A. B. Voitkiv, K. Schneider, X. Wang, A. C. Laforge, R. Hubele, J. Goullon, N. Ferreira, A. Kelkar, M. Grieser, R. Moshhammer, J. Ullrich, and D. Fischer, *Phys. Rev. A* **88**, 022704

VITA

Sachin Sharma was born in Dharamshala, India. In May 2006, he received his Master of Science degree in Physics from Guru Nanak Dev University, Amritsar, India. In Fall 2008, he joined Department of Physics in Missouri University of Science and Technology, Rolla, USA. Here, he worked as Graduate Teaching Assistant from Fall 2008 till Spring 2010. He was awarded Outstanding Teaching Assistant in Fall 2009 and Spring 2010. He received his Masters degree in Physics major in Summer 2011. In Fall 2011, he enrolled for Ph. D. degree in Department of Physics, Missouri University of Science and Technology. Here, he joined LAMOR (Lab for Atomic, Molecular & Optical Physics) for experimental investigation of Few-Body Problem. In December 2014, he received his Ph. D. in Physics from Missouri University of Science and Technology, Rolla, Missouri, USA.

Sachin has published six journal papers, four of which are part of this dissertation. He has presented his research work in Gaseous Electronic Conference (GEC) in 2011, 2012 and 2013. In GEC-2012 and GEC-2013, he was selected as a nominated speaker for Student Award of Excellence. In Spring 2012, he was awarded 1st prize for poster presentation in Graduate Research Showcase at Missouri University of Science and Technology, Rolla, USA. In December 2012, he was awarded 1st prize in Annual Shearer Prize for Research by Department of Physics. He has been a member of American Physical Society since 2012.